

# Metal clusters as a new application field of nuclear-physics ideas and methods

V. O. Nesterenko

*Joint Institute for Nuclear Research, Dubna*

Fiz. Elem. Chastits At. Yadra **23**, 1665–1714 (November–December 1992)

The physics of metal clusters is reviewed. It was recently established that metal clusters, which are bound systems of atoms of certain metals, have shells of the same type as atoms and nuclei. Subsequent investigations revealed a striking similarity of metal clusters and nuclei in many properties (shells, quadrupole deformation, fission, giant resonances, etc.). As a result, many of the ideas and methods of nuclear physics, in the first place theoretical, can, after a certain modification, be used to study the clusters. On the other hand, they have some unique properties (the possible formation of systems with up to 20 000 particles, supershells, mixed clusters). The physics of metal clusters, which relates to many disciplines (atomic and nuclear physics, quantum chemistry, solid-state physics, etc.), is a very promising direction from the point of view of both fundamental results and practical applications.

## 1. INTRODUCTION

As presently understood, the physics of metal clusters arose comparatively recently, in 1984, when it was found that the atoms of some metals (in the first place, alkali and noble) can form bound systems possessing an important property hitherto unknown in atomic clusters. Namely, in the experiments of Knight *et al.* (for sodium and potassium),<sup>1–4</sup> and also in the experiments of Katakuse *et al.* (for copper, silver, gold, cesium, and zinc)<sup>5</sup> it was shown that in metal clusters there exist shells, possessing, moreover, the same magic numbers as nuclei and atoms. At practically the same time, the West Berlin theoretician Ekardt<sup>6</sup> predicted shells in metal clusters. This very important discovery meant that, besides the atom and the nucleus, there exists in nature another small bound system possessing a mean field—the metal cluster. The valence (outside closed shells) electrons move in the mean field of the cluster. It will be shown below that it is the valence electrons that determine many properties of the clusters.

Because of the shells, metal clusters have many properties in common not only with a solid but also with atoms and nuclei. Accordingly, the physics of these objects is an interdisciplinary science at the frontier of atomic and nuclear physics and also solid-state physics, thermodynamics, crystallography, etc. Such a situation is very promising, since it is known that some of the most interesting results are often obtained where different fields of study meet. On the other hand, as will be shown below, metal clusters resemble nuclei in numerous properties. As a result, quite a lot of the ideas and methods (in the first place, theoretical ones) of nuclear physics can, after some modification, be effectively used to study the clusters.

Unfortunately, information about metal clusters is distributed over many journals of different directions and often requires special knowledge to be mastered. This makes it quite difficult to learn about them. There are some reviews<sup>7–10</sup> on individual directions in the field. The review of Ref. 7, published in 1987, gives a good picture of some

of the general properties of metal clusters and the methods by which they are obtained experimentally. However, that review covers only the first stages in the development of the field. Several directions that are currently developing very strongly, for example, giant resonances in the clusters, supershells, and clusters with a large number of particles, are not represented at all. To some extent, one can regard as a review the beautiful paper of Bjørnholm,<sup>8</sup> which reveals the interconnections between metal clusters and other types of cluster, in particular those constructed from helium atoms, which, according to theoretical predictions, must also have a mean field and nuclear-type shells. In Ref. 8, metal clusters are treated as links that make it possible to follow the transition from atoms to solids and to understand the stage at which a cluster is already an “embryonic” solid possessing its basic properties. In Kresin’s review,<sup>9</sup> collective properties of metal clusters are described. The exposition is mainly based on a modified Thomas–Fermi method.

In the first place, this review is intended for the reader who knows practically nothing about the physics of metal clusters but who wishes to acquire a general idea about its present status without going into details. In contrast to the earlier reviews, the aim of this one is to be a simple and accessible guide to the basic properties and most topical directions in the field. Since metal clusters have much in common with nuclei, the properties of the two classes of objects will be continually compared in order to establish where the scientific techniques developed in nuclear physics can be used. The exposition is in a form fully accessible to specialists in nuclear physics. Some of the material presented in this review appears in Ref. 10.

Section 2 gives a general picture of metal clusters and compares them with systems like atoms, nuclei, and solids. Section 3 explains briefly the principles used to obtain metal clusters in experiments. Section 4 recounts the discovery of shells in metal clusters and the main prospects for the development of the physics of these clusters. Section 5 is devoted to the properties of the ground state of

metal clusters, and Sec. 6 to an investigation of the deformations in these systems. Section 7 considers collective excitations in them. In Sec. 8, there is a brief description of large clusters and supershells.

## 2. FIRST DESCRIPTION OF METAL CLUSTERS

As we have already said, metal clusters are bound systems of atoms of certain metals. In the first place, these are alkali (lithium, sodium, potassium, rubidium, cesium) and noble (copper, silver, gold) metals, the distinctive property of which is that their valence electrons are not localized in space (so-called conduction electrons). There is here a close analogy with nucleons in a nucleus, which can also, in a first approximation, be regarded as free (as is well known, the mean free path of a nucleon in a nucleus is of the order of the nuclear diameter).

It is convenient to regard a cluster as a system of valence electrons in the field of positively charged ions. For the solution of a large number of problems relating to alkali and noble metals, the lattice of positively charged ions can, to good accuracy, be replaced by a uniform distribution of positive charge over the volume of the cluster (jellium approximation). This greatly simplifies investigations. This approximation works best for sodium clusters. Because of this, and also because the sodium atom is monovalent (which greatly simplifies the analysis of the data), the majority of experimental and theoretical studies on metal clusters have been devoted to sodium clusters.

The forces that create metal clusters as bound systems have the same basis as chemical forces—the Coulomb interaction. However, the forces are not the same as the chemical ones. Indeed, a metal cluster is usually formed from atoms of one metal, and the number of atoms may reach hundreds or thousands. On the other hand, it is known that through chemical forces the atoms of a given metal can be bound only in the simplest (for example, diatomic) molecules. Without going into details, the nature of the forces that bind the atoms in metal clusters can be demonstrated in a simplified form for the example of van der Waals forces. Their form is readily obtained by conceiving the Coulomb interaction between neutral atoms as the interaction between dipoles (formed by an electron and a positively charged ion).<sup>11</sup> Van der Waals forces are attractive. In contrast to chemical forces, which decrease exponentially with distance, the van der Waals forces have a  $1/R^6$  radial dependence, i.e., they have a greater range than chemical forces.

Valence electrons are the most important part of metal clusters. They determine many of their properties. In support of this, we can give the estimate of Ref. 8 deduced from the uncertainty relation:

$$\Delta x \Delta p \geq \hbar. \quad (1)$$

The expression (1) gives lower bounds for the momentum and energy of a particle in the system:  $\Delta p = \hbar/\Delta x$  and  $\Delta E = (\Delta p)^2/2m$ , respectively. For example, let us consider a neutral cluster consisting of 20 sodium atoms and possessing diameter 11.5 Å (1 Å =  $10^{-10}$  m). The valence electrons and positively charged ions are concentrated

within the cluster, and, therefore, for both of them  $\Delta x \leq 11.5$  Å. However, the masses of the electrons and ions differ strongly. Therefore

$$\Delta E_e \geq 0.16 \text{ eV for electrons,}$$

$$\Delta E_i \geq 0.04 \cdot 10^{-4} \text{ eV for ions.}$$

The temperature in a cluster is between 300 and 800 °K, corresponding to the interval  $kT = 0.03\text{--}0.08$  eV. It can be seen from this that the energy of the quantum motion of the ions is negligibly small compared with the temperature, i.e., the ions must behave as classical particles. In contrast,  $\Delta E_e > kT$ . Therefore, the behavior of the cluster as a quantum object will be determined by the valence electrons.

It is interesting to compare the properties of metal clusters with those of atoms, nuclei, and three-dimensional solids. The comparison will show why the clusters most strongly resemble nuclei.

### Metal clusters compared with atoms

*Similarity.* In both cases, the basic forces derive from the Coulomb interaction.

*Differences.* a) The atom behaves as a quantum gas: In going from light to heavy atoms, the volume of the atom changes little, while its density increases. In contrast, an increase in the number of particles in a metal cluster leads to an increase in the volume of the cluster and almost no change in its density. b) In an atom, the positive charge is concentrated at the center, while in a metal cluster it is distributed fairly uniformly over the complete volume.

### Metal clusters compared with nuclei

*Similarities.* a) Both the valence electrons in metal clusters and the nucleons in a nucleus can, in a first approximation, be regarded as free particles. Also, in both systems: b) the density remains practically unchanged with increasing number of particles; c) the charge is distributed relatively uniformly over the volume; d) surface effects play an important part; e) there is a quadrupole deformation in the case of open shells.

*Differences.* a) The types of interaction are different. b) The nucleus always has a positive charge, while a metal cluster can be either charged or neutral. c) In metal clusters, at least in the small and medium-sized ones, the spin-orbit interaction is negligibly small. d) As yet there is no unambiguous evidence for the existence of pairing in metal clusters.

### Metal clusters and three-dimensional solids

*Similarities.* There is a close connection between the properties of a metal cluster and the corresponding solid. The connection can be traced in properties such as the frequency of dipole vibrations, the polarizability, ionization potential, etc. The connection is due to the fact that the cluster, as a small part of a solid, retains some of its



most important properties. For example, the density of the atoms in a metal cluster and in the corresponding solid is practically the same.

*Differences.* a) The metal cluster is a system with diameter small compared with a solid. Therefore, the cluster has many properties absent in the solid (shells, deformation, fission, important role of surface effects, etc.).

b) The geometrical arrangement of the ions in a metal cluster is very different from the ionic lattice of the solid (see, for example, Ref. 12). It undergoes a complicated evolution with increasing number of atoms in the cluster, beginning with a large diversity of shapes for small clusters and ending, when there is a sufficiently large number of atoms in the cluster, with an ionic lattice of cubic type, as in the solid.

c) As already noted above, the forces that bind the atoms in the cluster are not the ordinary chemical forces.

### Specific properties of metal clusters

A metal cluster can be regarded as a small metallic droplet. Therefore, in charged metal clusters the charge is distributed over the surface. For a metal cluster, there is a screening effect. If one is placed in a static uniform electric field, it will behave as a dipole because of the redistribution of the charge.

Metal clusters can contain many more atoms than atoms can contain electrons and nuclei can contain nucleons.

Metal clusters can be of mixed type, i.e., composed of atoms of different elements.

From what we have said above, it can be seen that metal clusters are systems that, on the one hand, have quite a lot in common with atoms, nuclei, and solids but, on the other, possess numerous specific properties of their own. For our purposes, the most important thing is that, by virtue of some of the properties (presence of free valence electrons, constancy of the density, uniform charge distribution, importance of surface effects, etc.), metal clusters strongly resemble nuclei. As a result, numerous ideas and models developed in nuclear physics can be effectively used to study metal clusters.

We give the characteristic values of some physical quantities for metal clusters. The radius is given by

$$R = r_{ws} N^{1/3}. \quad (2)$$

Here,  $N$  is the number of atoms in the cluster,  $r_{ws}$  is the Wigner-Seitz radius, which is determined by the formula  $n^+ = (4/3\pi r_{ws}^3)^{-1}$ , where  $n^+$  is the density of the atoms in the solid. For sodium, for example,  $r_{ws} = 3.93$  a.u. (here and in what follows, we use atomic units of length: 1 a.u. =  $\hbar^2/me^2 = 0.529$  Å and of energy: 1 a.u. = 2 Ry = 27.2 eV). In accordance with (2), the radii of sodium clusters with  $N = 20$ –200 will be in the interval 5.6–12.2 Å.

The binding energy of a valence electron in a neutral cluster is on the average several electron volts. Metal clusters in the ground state (at temperature  $T = 0$  °K) are assumed to be stable. Experimental data on the lifetime of metal clusters in the ground state are not yet available. Calculations for the principal decay channel of neutral clusters—evaporation of atoms—indicate stability of them

at  $T = 0$  °K (see, for example, Ref. 12). Generally speaking, this question is nontrivial, since metal clusters can change their properties radically at low temperature (see Sec. 8).

### 3. THE PRODUCTION OF METAL CLUSTERS IN EXPERIMENTS

Many different methods can be used to obtain both free metal clusters and clusters implanted in a matrix. These methods are described in Ref. 7 and in several other studies (see, for example, Refs. 13 and 14). Each method has its advantages from the point of view of the problem posed (type of metal cluster, size, the experimental properties that are of interest, the reactions in which the clusters are investigated, etc.). Here, we shall present only a brief outline of the way in which the clusters are obtained and the measurements for them in experiments.

The simplest experimental facility includes: 1) a source of metal clusters; 2) a system that ionizes the beam (for example, ultraviolet light); 3) a quadrupole mass analyzer (Daley detector system), which, from the deflection of the ionized clusters in the magnetic field, determines their mass and, accordingly, the number of atoms in the cluster. The range of the beam is usually of the order of 2 m.

As an example, we consider a source of metal clusters with supersonic flow through a narrow nozzle (supersonic nozzle source).<sup>7</sup> In this source, the vapor of a metal, for example, sodium, is mixed with an inert gas. By regulating the temperature and pressure, the resulting mixture is brought to a state of “supersaturated vapor” and then passed through a narrow (0.0076 cm) nozzle into vacuum. The rapid expansion and cooling of the mixture which then occurs gives rise to a process of condensation type, and it is this that leads to the formation of the metal clusters. At the same time, the temperature of the clusters is quite low, as a consequence of which the beam of metal clusters is well focused.

In other methods, the clusters are obtained by evaporating the material by irradiating its surface with a laser or beam of heavy ions (for example,  $\text{Ar}^+$  with energy 10 keV). In the initial stage, the numbers of clusters of different sizes in the beam are more or less the same. However, at the end of the range, the situation is very different because of the intensive evaporation of atoms from the clusters. Since the evaporation rate depends on the binding energy of the atoms and therefore, for example, is very different for metal clusters with open and closed shells, the distribution of the clusters with respect to the number  $N$  of atoms is highly nonuniform at the end of the beam. It should be noted that modern experimental apparatus makes it possible to determine the number of atoms in a cluster rather accurately even for large clusters.

### 4. DISCOVERY OF SHELLS IN METAL CLUSTERS. THE PROSPECTS THAT ARE OPENED UP

As we already said in the Introduction, a decisive factor in the modern development of the physics of metal clusters was the discovery in them of shells having the

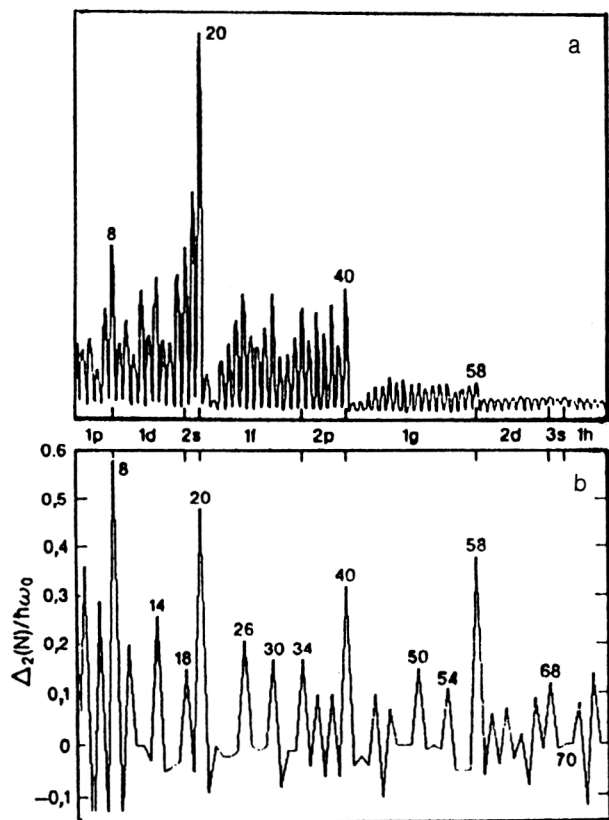


FIG. 1. Experimental abundance spectrum (a) giving the numbers (in relative units) of Na clusters in a beam as a function of the number  $N$  of atoms in the cluster.<sup>15</sup> For convenience, the abscissa gives the shells instead of  $N$ . The magic numbers are indicated directly in the figure. Figure 1b shows the function  $\Delta_2(N)$  calculated with the Nilsson potential.<sup>15</sup> For large peaks, the values of  $N$  are given.

same magic numbers as in nuclei and atoms.<sup>1-5</sup> Figure 1a shows the so-called abundance spectrum, which characterizes the relative number of sodium clusters in a beam as a function of the number of atoms in them.<sup>15</sup> Figure 1b shows the function

$$\Delta_2(N) = E(N+1) + E(N-1) - 2E(N), \quad (3)$$

which characterizes the relative change of the binding energy  $E(N)$  of a system containing  $N$  atoms compared with systems with  $N-1$  and  $N+1$  atoms (the binding energy was calculated for the Nilsson potential). As is well known,  $\Delta_2(N)$  is sensitive to the presence of a gap in the single-particle spectrum and has a peak for relatively stable systems.

It can be seen from Fig. 1 that the metal clusters with  $N=8, 20, 40$ , and  $58$  are strongly distinguished. These clusters are much more stable than their neighbors. Therefore, the numbers  $N=8, 20, 40$ , and  $58$  can be regarded as magic numbers. It is here extremely important that these magic numbers are equal to those in nuclei and atoms (a certain difference of them from the nuclear numbers, beginning with  $N=58$ , is explained by the fact that in a metal cluster, as in an atom, the spin-orbit interaction is negligibly small). The identity of the magic numbers indicates that metal clusters have the same mean field as in atoms and nuclei. In the mean field there are moving valence

electrons, which in this approximation can be regarded as not interacting with each other. The shells are also revealed in measurements of the ionization potential<sup>4</sup> and the static electric polarizability<sup>3</sup> of metal clusters.

Clusters with sets of magic numbers were known earlier.<sup>8</sup> For example, there are clusters formed from xenon atoms (or from atoms of other inert gases except helium) and possessing the magic numbers 13, 55, 147, 309, 561, and 923 (Refs. 8 and 16-18). There is also the famous  $C_{60}$  cluster, which is distinguished by particular stability for  $N=60$  and is a hollow sphere.<sup>19,20</sup> However, the values of the magic numbers of these clusters are different, and these values correspond to a quite different physics. For example, for Xe clusters, which are formed from atoms with closed electron shells, the above magic numbers reflect the geometry of the ion lattice. The Xe clusters have a shell structure of geometrical type corresponding to a family of icosahedrons. Here, the shells grow like the layers of an onion by the addition of new atoms to the surface of the cluster. The system becomes especially stable when the next icosahedron is formed by the addition of a sufficient number of atoms to the cluster.

Thus, the importance of the discovery of shells in metal clusters was that for the first time shells in clusters were found to have a nongeometrical nature. In this respect, the metal clusters are fundamentally different from other types of cluster. On the other hand, the type of shell makes them similar to atoms and nuclei. This stimulated a sudden burst of interest in metal clusters and gave a strong boost to experimental and theoretical investigations. A large amount of information on metal clusters has now been accumulated, the understanding of their properties has been deepened, and further prospects opened up. We shall attempt to outline briefly these prospects in order to show the respects in which the clusters are interesting in addition to the possession of shells.

Metal clusters with up to 3000 atoms are already being intensively investigated.<sup>21-24</sup> Clusters with  $N \leq 20\,000$  are known.<sup>25</sup> Thus, there is opened up for the first time a unique possibility for studying a continuous transition from a single atom (through a metal cluster) to a three-dimensional solid. Since small clusters behave as quantum objects, and large ones as classical objects, metal clusters provide a possibility for studying the transition from quantum-mechanical behavior of a system to classical behavior.

Besides shells, it was also predicted<sup>21,22</sup> and then confirmed experimentally<sup>23</sup> that metal clusters contain supershells. In accordance with Refs. 21 and 22, supershells can exist only in sufficiently large systems ( $N \geq 1000$ ). It is clear that this effect is in principle impossible in both atoms and nuclei.

Like nuclei, metal clusters can be deformed. The experiments have revealed clear signs of quadrupole deformation (characteristic peaks in the abundance spectrum,<sup>15</sup> splitting of a giant dipole resonance in a photoabsorption reaction<sup>26,27</sup>). There are theoretical predictions of the possible existence in metal clusters of other forms of deformation:  $\gamma$  deformation,<sup>26</sup> hexadecapole,<sup>28,29</sup> and

octupole.<sup>29,30</sup> It should be said that metal clusters present unique possibilities for studying different forms of deformation. In nuclei the number of nucleons is limited to a maximum of 300, but in metal systems one can study deformation with a much greater number of particles.

Deformed metal clusters can rotate. The rotation of clusters with a small number of atoms must be similar to the rotation of molecules. Large deformed metal clusters have a huge (on nuclear scales) moment of inertia, as a result of which they may reach high (hundreds of  $\hbar$ ) angular momenta already at very low angular velocities. However, the experimental observation of rotation of the clusters is very difficult, since the energy separation between neighboring rotational levels must be of order  $10^{-6}$ – $10^{-5}$  eV, whereas the temperature characteristic of the clusters reaches  $10^{-2}$ – $10^{-1}$  eV.

It has been established experimentally that positively charged metal clusters can, like nuclei, undergo spontaneous fission.<sup>31,32</sup> The fission can be investigated both in the framework of Strutinsky's shell-correction method<sup>33,34</sup> (see, for example, Ref. 35) and in a number of other approaches.<sup>36–38</sup> It is already possible<sup>32</sup> to obtain clusters with charge +14. At the same time, the critical value of  $Z^2/N$  was found<sup>32</sup> to be 1/8, in contrast to nuclei, for which  $Z^2/A \sim 49$ .

The question of the presence of pairing between valence electrons in metal clusters is of great interest.<sup>39,40,112</sup> Assertions of the presence of pairing in metal clusters are based on the experimentally detected even-odd difference in the ionization potential (the minimum energy needed to remove an electron from a cluster).<sup>41–44</sup> In sodium clusters, an even-odd difference in the ionization potential is observed<sup>44</sup> in a wide interval  $2 < N < 60$ . Unfortunately, in contrast to nuclei, in which information about pairing can be obtained from a quite wide range of experimental data (energy gap in even-even nuclei, moments of inertia, two-nucleon transfer reactions, even-odd differences in the binding energy), only the even-odd difference in the ionization potential can currently provide such data for metal clusters. Factors such as quadrupole deformation and rearrangement of the mean field on the transition from a neutral even cluster to a charged odd cluster explain the experimental data<sup>44</sup> only in part.<sup>45</sup> The discovery of pairing in metal clusters could have far-reaching consequences: competition between pairing and deformation, possible connections with high-temperature superconductivity, etc. Studies on high-temperature superconductivity show that various pairing mechanisms are possible, including the well-known interaction of electrons with positively charged lattice ions.

In metal clusters a giant  $E1$  resonance is observed experimentally (see, for example, Refs. 26, 27, and 46). It is found in clusters of the most varied types: small and large, spherical and deformed, neutral and charged. At the same time, depending on the type of cluster, the  $E1$  resonance has specific properties. It has been mainly investigated in the photoabsorption reaction,<sup>26,27</sup> although there are also data on the  $E1$  resonance in the optical spectra of metal clusters<sup>47</sup> and in reactions with electrons (see, for example,

Ref. 13). As yet, there are no reliable experimental data on giant resonances of other multipolarity.

There have been many theoretical studies of the properties of both electric and magnetic giant resonances of different multiplicities.<sup>49–72</sup> These studies have largely been predictive in nature.

As already noted, the experimentally obtained metal clusters have a quite high temperature (100–800 °K). The main channel of deexcitation and decay of the clusters is then evaporation of atoms.<sup>73</sup> In this respect, the clusters are very favorable objects for investigating a variety of statistical and thermal effects in quantum systems.<sup>68,73,74</sup>

Clusters of mixed type, i.e., possessing admixtures of atoms of other elements, can exist.<sup>7,75</sup> The study of mixed metal clusters is of great independent interest. Practical applications are here possible (new materials).

Metal clusters are particularly attractive for anyone who is concerned with theoretical nuclear physics. Because the clusters resemble nuclei in many of their properties, many models and approaches known in nuclear theory can, after some modification, be used to study the clusters. At the present time, wide use is already made of the single-particle potentials that have proved themselves well in nuclear physics: Nilsson<sup>15,45,76</sup> and Woods-Saxon.<sup>21,22,28,29</sup> Other models include the BCS model,<sup>39</sup> the vibrating-potential model,<sup>50,51</sup> the sum-rule method,<sup>49–56</sup> the random-phase approximation (Refs. 50, 51, 57–63, and 72), various forms of self-consistent calculations,<sup>65–69,77</sup> models of hydrodynamic type,<sup>51,71</sup> algebraic models like the interacting-boson model,<sup>40,79</sup> the liquid-drop model and the shell-correction method,<sup>29,35,80</sup> relativistic models,<sup>81</sup> the shell model (calculations of giant resonances),<sup>82,83</sup> etc. On the other hand, for nuclear theory models introduced into the physics of metal clusters from atomic physics and solid-state physics could be very interesting.

## 5. GROUND-STATE PROPERTIES OF METAL CLUSTERS

One of the most important characteristics of metal clusters is the density of valence electrons in the ground state:  $n_0(\mathbf{r})$ . This quantity determines many properties of the clusters and is an input element in the overwhelming majority of theoretical calculations.

The so-called jellium model is used in many cases to calculate  $n_0(\mathbf{r})$ . The essence of this is to ignore the lattice structure of the positively charged ions. In the jellium model, the lattice distribution of the ions in a metal cluster is replaced by a uniform distribution with a sharp boundary:

$$n^+ = n_{\text{bulk}}^+ \Theta(r - R), \quad (4)$$

where  $R$  is determined by the expression (2). The field of the ions is treated as an external field for the gas of valence electrons. The jellium approximation has proved itself well in the investigation of systems with free electrons, in particular in clusters formed from atoms of alkali metals.

The electron density  $n_0(\mathbf{r})$  is found by minimizing the energy functional  $E\{n_0(\mathbf{r})\}$  of the system. According to a theorem proved by Kohn, Sham, and Hohenberg,<sup>84,85</sup> the

functional  $E\{n_0(\mathbf{r})\}$  is unique if the exact energy is considered. However, for practical calculations of  $n_0(\mathbf{r})$  in

metal clusters one uses the so-called Kohn–Sham functional:

$$E\{n_0(\mathbf{r}), \tau(\mathbf{r})\} = \frac{1}{2} \int \tau(\mathbf{r}) d\mathbf{r} - \frac{3}{4} \left(\frac{3}{\pi}\right)^{1/3} \int n_0(\mathbf{r})^{4/3} d\mathbf{r} - \int \frac{0.44n_0(\mathbf{r})}{7.8 + (3/4\pi n_0(\mathbf{r}))^{1/3}} d\mathbf{r} + \frac{1}{2} \iint \frac{n_0(\mathbf{r})n(\mathbf{r}')}{|\mathbf{r}-\mathbf{r}'|} d\mathbf{r} d\mathbf{r}' + \int V_j n_0(\mathbf{r}) d\mathbf{r} + E_{jj}. \quad (5)$$

The terms of (5) are, respectively, the kinetic energy of the system, the Coulomb exchange term, the Lang–Kohn correlation term,<sup>86</sup> and also the direct Coulomb interaction of the valence electrons with each other, of the valence electrons with the positively charged ions, and of the positively charged ions with each other. In the Kohn–Sham approach, the kinetic energy and density of the valence electrons are expressed in terms of the single-particle electron wave functions  $\phi_i$ :

$$\tau(\mathbf{r}) = \sum_{i=1}^N |\nabla \phi_i|^2, \quad (6)$$

$$n_0(\mathbf{r}) = \sum_{i=1}^N |\phi_i|^2. \quad (7)$$

In the Thomas–Fermi approximation,

$$\tau(\mathbf{r}) = \frac{3}{5} (3\pi^2)^{2/3} n_0(\mathbf{r})^{5/3} + \frac{\beta (\nabla n_0(\mathbf{r}))^2}{4n_0(\mathbf{r})}, \quad (8)$$

and the functional (5) depends only on the density  $n_0(\mathbf{r})$ . In (8), the parameter  $\beta$  is chosen to reproduce on the average the results (5)–(7) in the Kohn–Sham approach.

By means of the variational procedure, it is easy to obtain from (5)–(7) and the normalization condition  $\int |\phi_i|^2 d\mathbf{r} = 1$  a system of equations for finding the single-particle wave functions:

$$\left[ -\frac{\nabla^2}{2} + v(n_0(\mathbf{r}), \mathbf{r}) \right] \phi(\mathbf{r})_i = \epsilon_i \phi(\mathbf{r})_i \quad (9)$$

with a corresponding form of the single-particle potential

$$v(n_0(\mathbf{r}), \mathbf{r}) = V_j(\mathbf{r}) + \int \frac{n(\mathbf{r}')}{|\mathbf{r}-\mathbf{r}'|} d\mathbf{r}' + \frac{dv_{\text{ex-corr}}}{dn_0}. \quad (10)$$

The exchange–correlation term in (10) has the form

$$v_{\text{ex-corr}} = -\frac{3}{4} \left(\frac{3}{\pi}\right)^{1/3} n_0(\mathbf{r})^{4/3} - \frac{0.44n_0(\mathbf{r})}{7.8 + (3/4\pi n_0(\mathbf{r}))^{1/3}}. \quad (11)$$

Equations (9)–(10) are solved iteratively.

It is interesting to note that the first two terms in (10) compensate each other to a large degree.<sup>12</sup> For a uniform density distribution of the valence electrons, there is complete compensation. In this case, the mean field (10) is completely determined by the exchange–correlation term (11). A screening effect of this kind occurs in the static

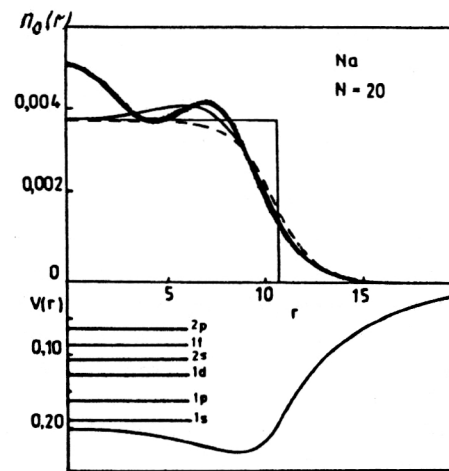
case. In the dynamic case, the situation is opposite. For example, in RPA calculations the residual interaction is mainly the Coulomb interaction, and its exchange–correlation part plays a comparatively secondary role.<sup>61</sup>

Figure 2 shows the electron density  $n_0(\mathbf{r})$  and the corresponding single-particle potential for the spherical  $\text{Na}_{20}$  cluster.<sup>53</sup> The electron potential is calculated in the microscopic Kohn approach, in the Thomas–Fermi approximation, and also using the two-parameter function

$$n_0(\mathbf{r}) = \frac{n_0}{1 + \exp[(r-R)/a]^\gamma}, \quad (12)$$

where the parameters  $n_0 = 3.73 \cdot 10^{-3}$  a.u.,  $\gamma = 1$ ,  $R = r_0 N^{1/3}$ ,  $r_0 = 3.9$  a.u., and  $a = 1.02$  a.u. were chosen on the basis of the condition of reproducing in the Thomas–Fermi approximation the results for Na clusters with  $N \geq 20$ . The larger the cluster, the better the function (12) reproduces the results of this approximation.

It can be seen from Fig. 2 that the microscopic calculation in the Kohn–Sham approach, in contrast to the last two approximations, gives oscillations in the interior region of the cluster, which are a reflection of its shell structure.





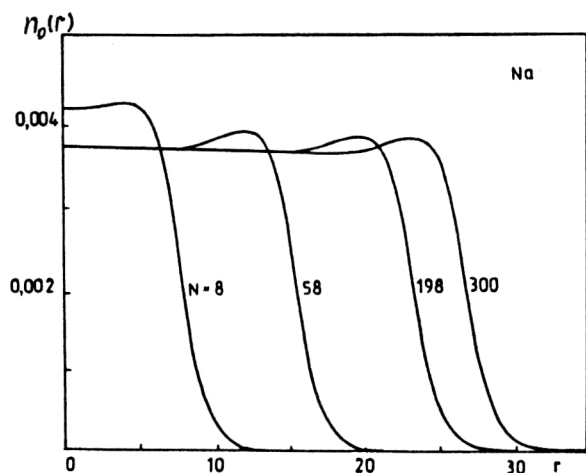


FIG. 3. Densities  $n_0(r)$  of valence electrons calculated in the Thomas-Fermi approximation for spherical Na clusters with  $N=8, 58, 198$ , and  $300$  (Ref. 53).

It can also be seen from Fig. 2 that the density  $n_0(r)$  has a fairly long tail outside the boundaries specified by the jellium model. This is the so-called spill-out effect (literally spilling of some of the valence electrons outside the jellium). This effect is extremely important for understanding the differences between the properties of metal clusters and a three-dimensional solid (see below). The number  $\delta n_0$  of electrons outside the cluster ( $r > R$ ) depends on the size of the cluster. For example,  $\delta n_0=1.5$  (19%) and  $9.5$  (7%) for  $N=8$  and  $138$ , respectively.<sup>12</sup>

Figure 3 shows the density  $n_0(r)$  calculated in the Thomas-Fermi approximation for some spherical Na clusters. The calculations show that with increasing  $N$  the density of valence electrons in the Na clusters hardly changes, beginning with  $N \geq 8$ . In this respect, the clusters are similar to nuclei, the density of which can also be regarded as practically constant.

An important characteristic of the cluster ground state is the electric polarizability  $\alpha$ , which is determined by the dipole moment  $p = \alpha E_0$  of the system produced by an external field  $E_0$ . In the classical limit,

$$\alpha_{cl} = R^3. \quad (13)$$

It is well known that the experimental values of  $\alpha$  appreciably exceed the classical limit, particularly for small clusters (see Fig. 4, which gives experimental data for Na and K clusters<sup>3</sup>). To a large degree, the excess is explained by the spill-out effect produced by the external field  $E_0$ .<sup>87</sup> Keeping the form of the expression (13), it is convenient to represent the static electric polarizability in the metal cluster in the form

$$\alpha = (R + \delta_\alpha)^3. \quad (14)$$

Table I gives the values of  $\delta_\alpha$  calculated in Ref. 87 for  $r_{ws}$  equal to 2 and 4 a.u. (this range basically covers the characteristic values of  $r_{ws}$  in metal clusters. It can be seen

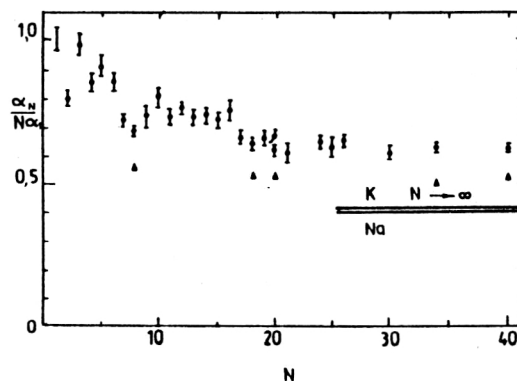


FIG. 4. Experimental data<sup>3</sup> on the static electric polarizability  $\alpha$  (per atom) for Na (black circles and black squares) and K (crosses) clusters. The data are normalized to the corresponding values of  $\alpha_1$  for the atoms.

from Table I that  $\delta_\alpha$  is almost independent of  $N$ . The values obtained for  $\delta_\alpha$  are close to those found for a semi-infinite metallic medium.<sup>87</sup>

Experiments also reveal the clear presence of shell effects in the dependence of  $\alpha$  on  $N$ .<sup>3,12</sup> This can be clearly seen in Fig. 4.

## 6. DEFORMATION OF METAL CLUSTERS

The presence of quadrupole deformation in metal clusters with open shells can be regarded as a well-established fact. Direct experimental evidence for quadrupole deformation like rotational bands in nuclei has not yet been observed in metal clusters. However, there are many rather convincing indirect indications. Quadrupole deformation is manifested in splitting of the giant dipole resonance in photoabsorption and photofragmentation reactions<sup>26,27,46</sup> (see Figs. 5 and 6). In addition, if quadrupole deformation is taken into account in calculations, one can significantly improve the description of experimental properties such as the abundance spectrum, the electric polarizability, the ionization potential, the dissipation energy (the minimum energy needed to separate an atom from a cluster), etc.<sup>15,45</sup>

Let us first consider the abundance spectrum in Fig. 1. Besides the high peaks corresponding to the magic numbers, there are also peaks of intermediate height (for example, the peak at  $N=14$ ). Since these peaks of intermediate height correspond to clusters with open shells, by analogy with nuclei it is natural to assume that they result from quadrupole deformation of the clusters. This question

TABLE I. Values of  $\delta_\alpha$  calculated in Ref. 87 for  $r_{ws}$  equal to 2 and 4 a.u.

$r_{ws}$	$R$	$N$	$\delta_\alpha$
2	4	8	1,921
2	7	43	2,014
2	14	343	2,029
2	40	8000	2,010
4	7	5	0,923
4	14	43	0,909
4	40	1000	0,886

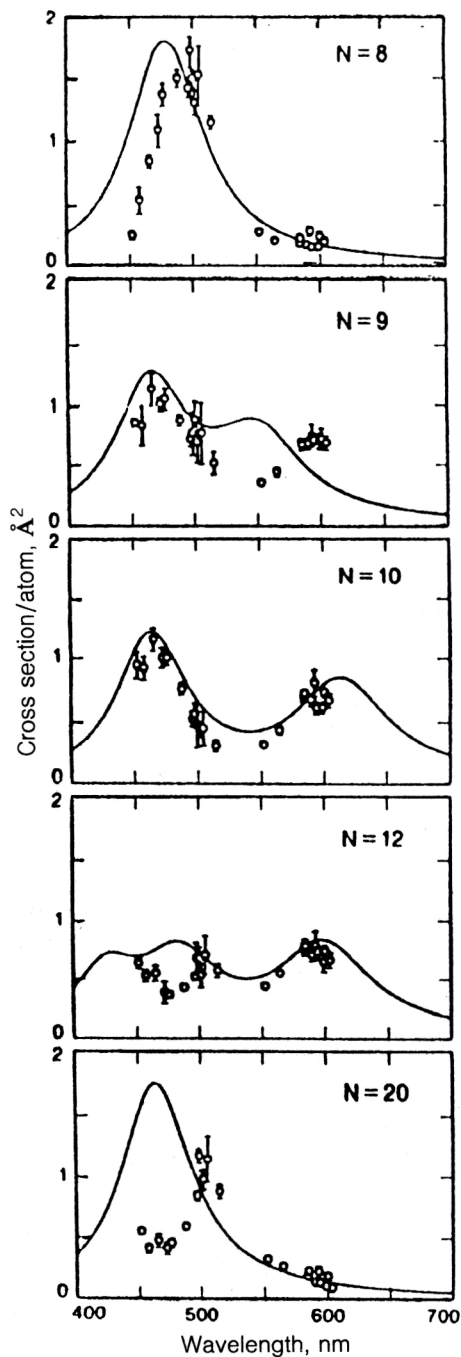


FIG. 5. Experimental (open circles) and theoretical (continuous curve) photoabsorption cross section for Na clusters with  $N=8-20$  (Ref. 26).

was investigated in a classical study of Clemenger,<sup>15</sup> who, to calculate the single-particle spectrum of a cluster, used the Nilsson single-particle spectrum,<sup>88,89</sup> which is well known in nuclear physics and corresponds to a system in the shape of an ellipsoid of revolution:

$$H = \frac{p^2}{2m} + \frac{1}{2}m\omega_0^2(\Omega^2(x^2 + y^2) + \Omega_z^2 z^2) - U\hbar\omega_0(l^2 - \langle l^2 \rangle_n), \quad (15)$$

where

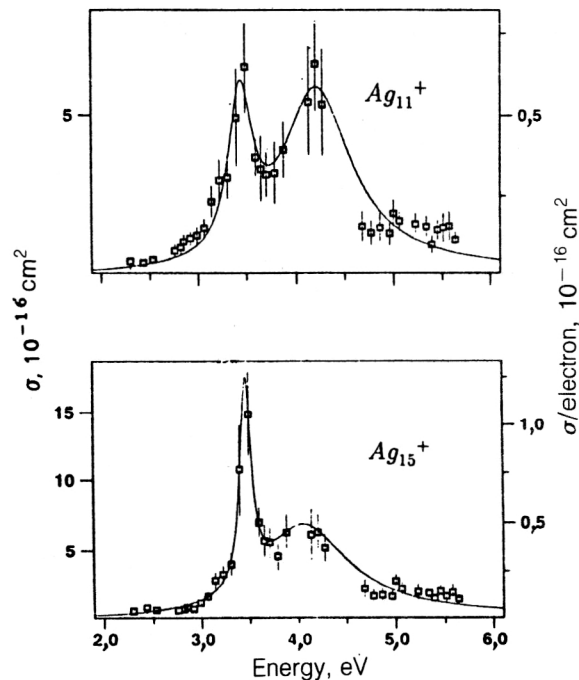


FIG. 6. Manifestation of giant  $E1$  resonance in the photofragmentation cross section for deformed  $Ag_{11}^+$  and  $Ag_{15}^+$  clusters.<sup>46</sup> The points are the experimental data; the continuous curves are from the calculation.

$$\langle l^2 \rangle_n = \frac{1}{2}n(n+1), \quad (16)$$

$$\Omega_1 = \left( \frac{2 + \delta_2}{2 - \delta_2} \right)^{1/3}, \quad (17)$$

$$\Omega_z = \left( \frac{2 + \delta_2}{2 - \delta_2} \right)^{-2/3}. \quad (18)$$

Then, under the condition of conservation of the volume,  $\Omega_1^2 \Omega_z = 1$ , the deformation parameter  $\delta_2$  can be expressed in terms of the semiaxes and mean radius of the ellipsoid of revolution:

$$\delta_2 \cong \frac{R_z - R_x}{R}. \quad (19)$$

There is no spin-orbit interaction in (15). The experimentally known sequence of magic numbers in metal clusters shows that this interaction can be ignored. The parameters  $U=0.34$  and  $\omega_0 \propto N^{-1/3}$  were chosen to reproduce the single-particle spectrum obtained in self-consistent calculations in the jellium model<sup>90</sup> (such a method of selecting parameters is used quite often, since experimental data on the single-particle spectrum are not available).

For different values of  $\delta_2$ , Clemenger calculated the binding energy of the Na clusters as the sum of the single-particle energies corresponding to occupied states. Equilibrium values of the quadrupole deformation were found for each  $N$  in the range  $N \leq 40$  by minimizing the binding energy with respect to  $\delta_2$ . The results are presented in the form of a Nilsson diagram in Fig. 7. They are given in dimensionless form in order to avoid choosing a specific value of  $\omega_0$ . The levels of the deformed clusters are characterized by the Nilsson quantum numbers  $nn_z\Lambda$ . Because



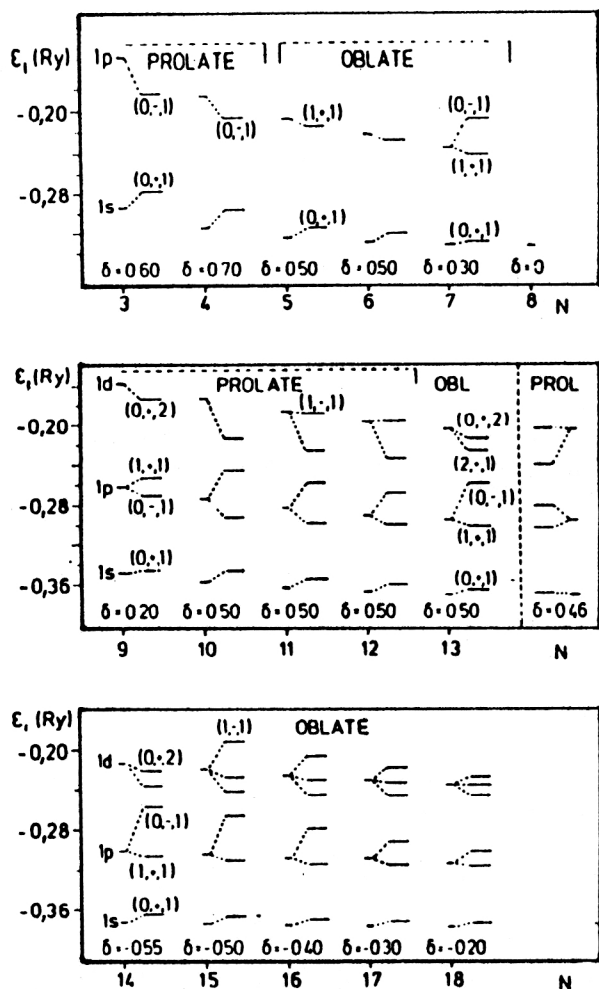


FIG. 8. Evolution of single-particle levels of Na clusters with  $3 < N < 18$  on the transition from spherical to deformed shape.<sup>45,76</sup> For each  $N$ , the rounded values of the quadrupole deformation parameter  $\delta$  obtained by a self-consistent calculation are given. For  $N=13$ , the results are given for both prolate and oblate deformations, since the energy of the system in the two cases is approximately the same.

$y_0$ , and  $z_0$  were found by minimizing the energy of the system. For  $N=12$  and  $16$ , shapes differing from an ellipsoid of revolution were obtained. For these clusters,  $x_0$ ,  $y_0$ , and  $z_0$  are, respectively,  $0.770$ ,  $0.963$ ,  $1.348$  and  $0.794$ ,  $1.058$ ,  $1.191$ . For  $N=10$ ,  $14$ , and  $18$ , the clusters have the shape of a spheroid, and the values of  $\delta_2$  are close to those obtained in Refs. 15, 45, and 76.

TABLE II. Values of the quadrupole and hexadecapole deformation parameters  $\delta_2$  and  $\delta_4$  calculated in Refs. 15, 26, 79, 45, 76, and 28.

$N$	$\delta_2$ [15]	$\delta_2$ [26]	$\delta_2$ [79]	$\delta_2$ [45,76]	$\delta_2$ [28]	$\delta_4$ [28]
8	0	0	0,043	0	0	0
10	0,44	0,44	0,074	0,48	0,27	0,11
12	0,43	—	0,167	0,5	0,33	-0,07
14	-0,49	-0,50	0,163	-0,56	—	—
16	-0,34	—	0,181	-0,4	—	—
18	-0,21	-0,24	-0,076	-0,2	—	—
20	0	0	-0,043	0	0	0

In Ref. 79, the values of  $\delta_2$  were calculated by requiring a description in the interacting-boson model of the splitting of the giant dipole resonance in the photoabsorption reaction for Na clusters.<sup>26</sup> Not only the quadrupole deformation but also the interaction of the dipole mode with the quadrupole vibrations was taken into account. In contrast to other studies, the values found for  $\delta_2$  are small. In addition, they are nonvanishing for the magic numbers  $N=8$  and  $20$ . It appears that one must take some care when extracting  $\delta_2$  from experimental data on the splitting of the giant dipole resonance. The splitting may be due to not only deformation but other factors. For example, the experimentally known splitting of the giant  $E1$  resonance in the spherical cluster  $\text{Na}_{20}$  is manifestly not associated with deformation. It is a typical configuration effect.<sup>61</sup>

In Refs. 45 and 76, calculations were made by the self-consistent method described in the previous section. In the Kohn-Sham functional (4), the field  $V_j$  of the ions was treated in the model of a spheroidal jellium. The equilibrium  $\delta_2$  was again taken to be the value at which the system had minimum energy. These calculations are of great interest, since the only input parameter here is the Wigner-Seitz radius  $r_{\text{WS}}$ . It can be seen from Table II that the self-consistent calculations give practically the same results as the simpler calculations of Refs. 15 and 26.

A single-particle Woods-Saxon potential with quadrupole and hexadecapole deformation<sup>94</sup> was considered in Ref. 28. The parameters of the potential (apart from the deformation parameters) were taken from Ref. 22, where they were chosen for a potential of this type from the condition of reproducing the results of Ekardt's self-consistent calculations.<sup>6</sup> The equilibrium values of the deformations were then found by minimizing the cluster energy. It can be seen from Table II that, compared with Refs. 15, 26, 79, 45, and 76, the results of these calculations (the values of  $\delta_2$  and  $\delta_4$  and their behavior as functions of  $N$ ) are closest to what we have in nuclear physics.

Summarizing the discussion of the results presented in Table II, we must point out that the actual fact of quadrupole deformation in metal clusters with open shells is in no doubt, but its value must still be determined more accurately. The inclusion of pairing may also influence the magnitude of the deformation. The above results relate to neutral clusters. For charged clusters, deformation calculations have not yet been made.

Quadrupole deformation influences many properties of



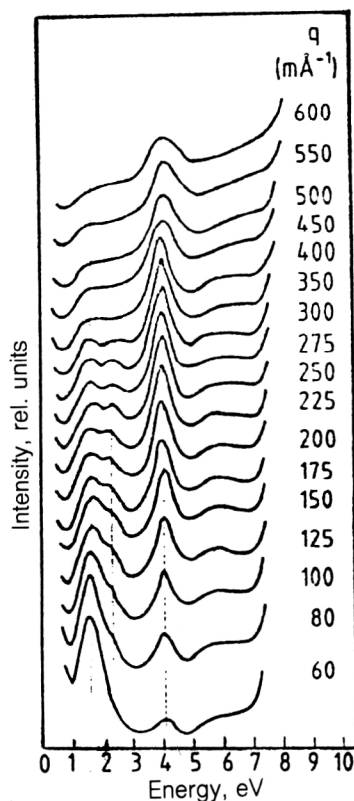


FIG. 9. Spectrum of K clusters obtained by electron-energy-loss spectroscopy.<sup>13</sup>

metal clusters with open shells. Besides what we have said above, we note that deformation increases the electric polarizability. In accordance with Ref. 15, the polarizability in deformed clusters, averaged over all directions, has the form

$$\bar{\alpha} = \bar{\alpha}_{\delta_2=0} \left(1 + \frac{4}{9} \delta_2^2\right). \quad (21)$$

To conclude this section, we note that the study of deformation in metal clusters is one of the most promising directions. There is interest in looking for quadrupole superdeformation or exotic forms of deformation in metal clusters.<sup>30</sup> We do not know what deformation large clusters possess, nor what are the global trends in the variation of the deformation with increasing number of atoms in the clusters. In metal clusters, the deformation is realized under conditions different from those in a nucleus (charge neutrality of the cluster, absence of spin-orbit interaction, etc.), and therefore we can here expect results different from those that we have for nuclei.

## 7. COLLECTIVE EXCITATIONS IN METAL CLUSTERS

There have been numerous studies, both experimental and theoretical (Refs. 13, 26, 27, and 46–75) devoted to collective excitations (giant resonances) in metal clusters. The giant dipole resonance has been studied well experimentally in the photoabsorption and photofragmentation reactions (see, for example, Refs. 26, 27, and 46 and Figs. 5 and 6). Many theoretical studies have also been devoted

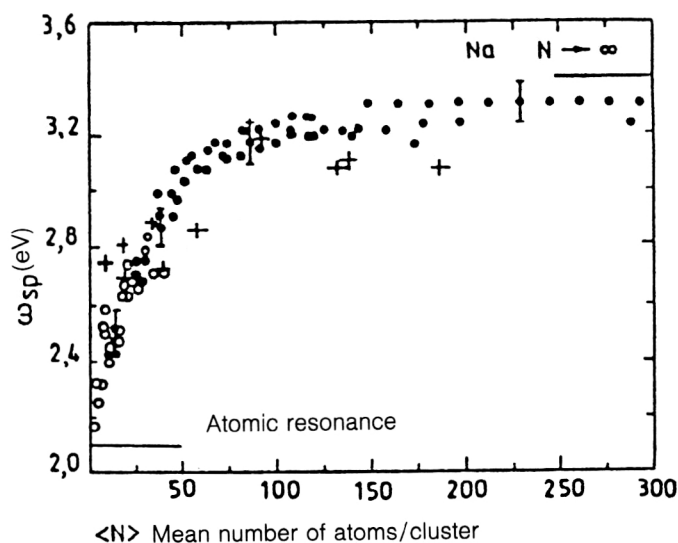


FIG. 10. Optical spectrum of Na clusters (Ref. 51): the black symbols are the experimental data of Ref. 47, the open circles are the frequencies calculated by the sum-rule method using data for the static polarizability (Ref. 3), and the crosses are the results of the calculations of Ref. 105.

to this resonance. There have been investigations (Refs. 13, 54, 56, 70, 96 and 97) (including experimental ones, Refs. 13, 96, and 97; see Fig. 9) of the manifestations of giant electric resonances of surface and bulk type in electron reactions (electron-energy-loss spectroscopy). We note, however, that experimental information on giant resonances with  $\lambda > 1$  is as yet very uncertain and imprecise. There are recently published experimental data on collective dipole excitations obtained from optical spectra of metal clusters<sup>47</sup> (see Fig. 10). With regard to collective excitations of magnetic type, there are here only theoretical predictions of the existence, in deformed clusters, of a low-lying resonance of "scissor" type<sup>39,40</sup> like what is found in nuclei.<sup>95</sup> As yet there are no experimental data on giant resonances of magnetic type.

Many different approaches are used to describe giant resonances in metal clusters (see the references in Sec. 3). This is practically the same set of models and approaches as is used to study giant resonances in nuclei. Small clusters ( $N < 8$ ), whose excitations are also investigated in the framework of quantum-chemistry models, constitute something of an exception. The basis of these models is a search for a cluster geometry for which the cluster energy is a minimum (see the review of Ref. 106). In a single section, it is not possible to cover all the material on giant resonances in metal clusters. Therefore, we shall describe here only their main properties, using the results obtained in the four most actively used approaches: the sum-rule method,<sup>50–56</sup> the random-phase approximation (RPA),<sup>48,57–64,72</sup> the linear response-function method,<sup>65–69</sup> and the approach of Kresin.<sup>9,57,58</sup>

### Sum-rule method

We consider the description of giant resonances in the sum-rule method, recalling first the basic propositions of

this method.<sup>98</sup> The main role is played by sum rules  $m_k$ , which are defined as moments of the strength function  $S(E)$ :

$$m_k = \int E^k S(E) dE = \sum_n E_n^k |\langle n | Q | \rangle|^2, \quad (22)$$

where

$$S(E) = \sum_n \delta(E - E_n) |\langle n | Q | \rangle|^2, \quad (23)$$

$Q$  is the external field,  $E_n$  and  $|n\rangle$  are the energies and wave functions of the excited states, and  $|\rangle$  is the ground-state wave function.

It is known that the odd moments  $m_k$  can be calculated to RPA accuracy in which they are expressed in terms of the commutators of the Hamiltonian and the operator  $Q$  using the bra and ket of the ground state of the system. It is sufficient to take the ground state in the Hartree-Fock approximation. For example, the expressions for the moments  $m_1$  and  $m_3$  are expressed as

$$m_1 = \frac{1}{2} \langle [Q, [H, Q]] \rangle, \quad (24)$$

$$m_3 = \frac{1}{2} \langle [[H, [H, Q]], [H, Q]] \rangle. \quad (25)$$

The approximation of a local density plays an important role in the sum-rule method. In it, only the term of the Hamiltonian corresponding to the kinetic energy of the system contributes to the commutator  $[H, Q]$  in the expressions (24) and (25). Determining the functions

$$E_k \equiv (m_k / m_{k-2})^{1/2}, \quad (26)$$

we can obtain upper and lower bounds for the excitation energy of the giant resonance and an upper bound for its variance:

$$E_1 \leq \bar{E} \leq E_3, \quad (27)$$

$$\sigma^2 \leq \frac{1}{4} (E_3^2 - E_1^2). \quad (28)$$

Thus, if we know the ground-state wave function of the system in the single-particle approximation, the sum-rule method enables us to estimate the basic properties of the giant resonance to the accuracy of the RPA without having to solve the complete set of RPA equations. In this respect, the simplicity of the method is attractive, and this is particularly important when one is considering large clusters. A shortcoming of the method is its basic approximation—that the entire strength of a given multipolarity is concentrated in a single collective state. Therefore, the method cannot be used, for example, to study the fragmentation of collective states.

We consider a metal cluster whose valence electrons are described by the Hamiltonian (in the system  $e = m_e = \hbar = c = 1$ )<sup>50</sup>

$$H = \sum_i \frac{p_i^2}{2} + \frac{1}{2} \sum_{i < j} \frac{1}{|\mathbf{r}_i - \mathbf{r}_j|} + \sum_i V_{\text{ext}}(\mathbf{r}_i), \quad (29)$$

where the first term is the kinetic energy, the second is the Coulomb interaction of the electrons with each other, and the third is an external field representing the interaction of

the ions with the electrons. Poisson's equation relates  $V_{\text{ext}}$  to the density of the positively charged ions:

$$\nabla^2 V_{\text{ext}} = 4\pi n^+(\mathbf{r}). \quad (30)$$

In the case of dipole excitations, when  $Q(\mathbf{r}) = x, y, z$ , we have

$$[H, Q] = -\frac{i}{2} P^{(k)}, \quad (31)$$

where  $P^{(k)} = \sum_i p_i^{(k)}$  is the  $k$ th component of the total angular momentum of the valence electrons ( $k = x, y, z$ ). Substituting (31) in (24) and (25), we obtain for the moments the expressions

$$m_1 = \frac{N_e}{2}, \quad (32)$$

$$m_3 = \frac{1}{2} \int d\mathbf{r} \nabla^2 V_{\text{ext}}(\mathbf{r}) n_0(\mathbf{r}), \quad (33)$$

where  $N_e$  is the number of valence nucleons in the cluster.

Note that the expression for  $m_1$  is the same for all three components of the dipole operator. It is determined by the number of valence electrons. It is also important to note that the expression for  $m_3$  does not depend on the interaction between the electrons, since this interaction, in contrast to  $V_{\text{ext}}(\mathbf{r})$ , commutes with the total angular momentum  $P^{(k)}$ . This effect occurs only in the case of a dipole external field.

It was shown in Ref. 99 that in the approximation of a local density the terms of the energy functional having a bulk nature (depending only on the electron density), namely, the exchange-correlation term, do not contribute to  $m_3$ . Therefore, the properties of giant resonances in metal clusters will, in general, be determined solely by the contribution of the kinetic energy and the direct Coulomb interaction.

In obtaining the expressions (32) and (33), we did not make any assumptions about the cluster shape. Therefore, they are true for both spherical and deformed clusters. But if we do assume a spherical shape, then the expression (33) takes, with allowance for Poisson's equation (30), the even simpler form

$$m_3 = \frac{2\pi}{3} \int dr n^+(r) n_0(r). \quad (34)$$

Such an expression for  $m_3$  was obtained earlier for atoms.<sup>100</sup> A general expression for the sum rule  $m_3$  of dipole transitions in finite Fermi systems (nucleus, atom, metallic particle), which determines the excitation energy of the giant dipole resonance in these systems, was derived in Ref. 78.

On the basis of (26) and (27), we can estimate the mean energy of a giant resonance in spherical clusters as

$$\psi = \sqrt{\frac{m_3}{m_1}}. \quad (35)$$

If (35) is compared with the well-known expression for the frequency of a harmonic oscillator, then it is readily seen

that  $m_1$  and  $m_3$  are the mass parameter and rigidity parameter (restoring force). Then, on the basis of (35), it can be concluded that in the case of a giant dipole resonance the restoring force in a metal cluster is proportional to the overlap of the densities of the ions and of the valence electrons.

Further, from (32), (34), and (35) we obtain

$$\omega^2 = \frac{4\pi}{3} \frac{1}{N_e} \int dr n^+(r) n_0(r). \quad (36)$$

If we take the ion density in the jellium model (4), we finally have

$$\omega = \omega_{Mie} \left( 1 - \frac{1}{2} \frac{\delta N_e}{N_e} \right), \quad (37)$$

where

$$\omega_{Mie} = \sqrt{\frac{4\pi}{3} n^+(r)} = \frac{1}{\sqrt{3}} \omega_p \quad (38)$$

is the frequency of the dipole resonance for a classical charged droplet<sup>101</sup> ( $\omega_p$  is the plasma frequency), and

$$\delta N_e = \int_{r>R} dr n_0(r) \quad (39)$$

is the number of electrons outside the radius  $R$  [see (2)] specified by the ion distribution in the jellium model.

It can be seen from (37) that the presence of exterior electrons (spill-out effect) leads to a so-called red shift of the resonance frequency—it is reduced in relation to the classical value. This in part explains the known excess of the classical frequencies (38) over the experimental data (see, for example, Ref. 26).

A further important conclusion follows from (37): In contrast to nuclei and, as will be seen below, giant electric resonances with  $L > 1$  in metal clusters, the excitation energy  $\omega$  of a dipole resonance in a metal cluster does not decrease but increases with increasing  $N$ . The main reason for this is again the spill-out effect. Such a dependence of  $\omega$  on  $N$  is found experimentally for sodium clusters.<sup>26,27</sup> However, in clusters made from atoms of noble metals (for example, from silver atoms), where the influence of localized electrons is already significant, the experiments give the same dependence of the dipole frequency on  $N$  as in nuclei, namely,  $\omega$  decreases with increasing  $N$ .<sup>46</sup> As can be seen from Fig. 11, this tendency is not reproduced in calculations in which the localization of the electrons is not taken into account.<sup>53</sup>

Allowance for the spill-out effect makes it possible to improve significantly the description of the experimental excitation energy of the giant dipole resonance, although the theoretical values are still higher than the experimental ones (so-called blue shift). Other effects must be taken into consideration. As will be shown below, it is important here to go beyond the local-density approximation.<sup>55</sup> In conclusion, we note that the calculations (29)–(39) were taken from Refs. 50 and 51.

We now consider the results of Refs. 53 and 55, in which, for a number of spherical clusters, the sum-rule

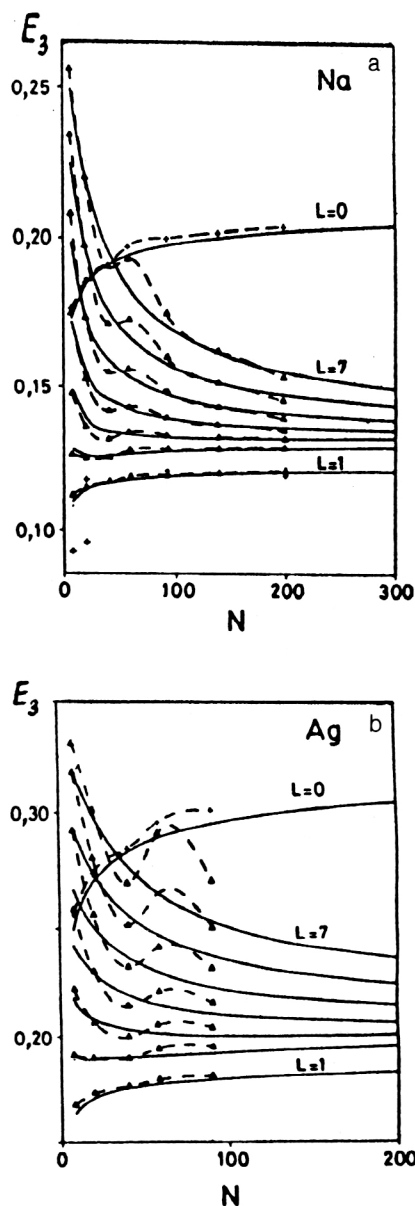


FIG. 11. Energies  $E_3$  (in a.u.) calculated for giant resonances with  $L=0-7$  in Na clusters with  $N=8, 20, 40, 58, 92, 138$ , and  $198$  in the framework of the Kohn-Sham approach (broken curves) and in the Thomas-Fermi approximation (continuous curves) (Ref. 53) (a). The same for Ag clusters with  $N=8, 20, 40, 58$ , and  $90$  (b).

method was used for numerical calculations of the excitation energies of giant electric resonances of different multipolarities, both in the local-density approximation<sup>53</sup> and going beyond this approximation.<sup>55</sup> The density  $n_0(r)$  of valence electrons in the ground state and the kinetic-energy density  $\tau(r)$ , which are the only unknowns in the expressions for the moments  $m_1$  and  $m_3$ , were calculated in two approaches: Kohn-Sham and Thomas-Fermi (see Sec. 5). The ion density was chosen in the jellium model. In this case, the ions cannot vibrate, and the giant resonances of any multipolarity in such a treatment are vibrations of the valence electrons with respect to the rigid ion medium. In such a treatment, the giant resonances in metal clusters differ from those in nuclei, in which both components of

TABLE III. The ratio  $(\delta N)_{\text{NLDA}}/(\delta N)_{\text{LDA}}$  and the electric polarizability  $\alpha$  calculated for  $\text{Na}_8$  and  $\text{Na}_{20}$  clusters in the local (LDA) and nonlocal (NLDA) approximations for the density of the valence electrons.<sup>55</sup> For comparison, the corresponding experimental data are given. The polarizability  $\alpha$  is given in units of  $\alpha_{\text{cl}} = R^3$  ( $R = r_{\text{WS}} N^{1/3}$ ,  $r_{\text{WS}} = 4$  a.u.).

Cluster	$\frac{(\delta N)_{\text{NLDA}}}{(\delta N)_{\text{LDA}}}$	$\alpha_{\text{LDA}}$	$\alpha_{\text{NLDA}}$	$\alpha_{\text{exp}}$
$\text{Na}_8$	1,40	1,45	1,18	1,72
$\text{Na}_{20}$	1,15	1,37	1,63	1,62

the system—the neutrons and the protons—participate in the vibrations.

Figure 11 gives the results of calculations of  $E_3$  [upper bound for the resonance excitation energy; see (26) and (27)] for some spherical Na and Ag clusters.<sup>53</sup> Resonances with  $0 \leq L \leq 7$  were considered. To analyze the results, it is convenient to use a simplified expression for  $E_3^2(L)$  obtained in Ref. 53 in the framework of the sum-rule method in the Thomas–Fermi approximation under the condition that the density of the valence electrons is also determined by the jellium model [ $n_0(r) = n^+(r) = n_{\text{bulk}}^+ \Theta(r - R)$ ]:

$$E_3^2(L) = \hbar^2 \omega_p^2 \frac{L}{2L+1} + \frac{2}{3} \hbar^2 (2L+1)(L-1) \frac{\beta^2}{R^2}, \quad (40)$$

where

$$\beta = \left(\frac{3}{2}\right)^{1/2} v_F = \left(\frac{3}{2}\right)^{1/2} (3\pi^2)^{1/3} \frac{\hbar}{m} n_0(r)^{1/3}. \quad (41)$$

In the expression (40), the first term arises from the Coulomb interaction [electron–electron ( $e$ – $e$ ) and electron–ion ( $e$ – $i$ )], while the second term derives from the kinetic energy of the system. As will be shown below, this expression, despite its simplified form, gives a basically correct behavior of the energies of the giant resonances as functions of  $L$  and  $N$ . In particular, there follows from it immediately our earlier conclusion that the dipole excitations ( $L=1$ ) are determined solely by the Coulomb interaction (more precisely, by the  $e$ – $i$  interaction).

Let us consider Fig. 11. It can be seen that for small clusters the excitation energies of the giant resonances of different multiplicities with  $L > 0$  differ strongly, and the higher the multipolarity, the higher the excitation energy. With increasing  $N$ , there is a basic tendency for  $E_3$  to decrease, and for large  $N$  the values of  $E_3$  corresponding to resonances of different multiplicities ( $L > 1$ ) collect into a pencil, tending to certain constant values. The expression (40) reflects this tendency. For fixed  $L$ , the contribution of the second term in it decreases with increasing  $N$  (and, accordingly, with increasing  $R$ ), whereas the first term remains constant.

In contrast to this tendency, the  $E_3$  for small multiplicities decrease comparatively weakly with increasing  $N$ . Moreover, in the case  $L=1$  there is an increase of  $E_3$  with increasing  $N$ . In Ref. 53, this behavior is explained by the diffuseness of the electron density  $n_0(r)$  at the cluster boundary [the spill-out effect; see (37) for dipole excitations]. It is clear that the influence of diffuseness will be

greatest for small clusters (and for small  $L$ , to decrease the competition with the main tendency determined by the second term in the expression (40)). The diffuseness of the electron density is not taken into account in (40), as a consequence of which the expression (40) does not describe these features.

It can also be seen from Fig. 11 that for Na clusters the values of  $E_3$  obtained in the quantum approach (Kohn–Sham), which takes into account shell effects, and in the semiclassical approach (Thomas–Fermi) are similar only for small and large  $N$ . In Ag clusters, the results are close to each other only for large  $N$ . Thus, as was to be expected, the Thomas–Fermi approximation, which gives a reasonable description of the general tendencies, the orders of magnitude, and also their numerical values at large  $N$ , cannot pretend to a quantitative description of clusters with  $N < 100$ , in which quantum effects are quite important. Here, it is necessary to use the Kohn–Sham approach.

Further, it was shown in Ref. 53 that, from a certain  $L$ , the contributions to  $m_3$  from the  $e$ – $e$  and  $e$ – $i$  interactions compensate each other, and  $E_3$  is determined solely by the contribution from the kinetic energy. This effect also follows from Ref. 40: With increasing multipolarity  $L$  for fixed  $N$  the second (kinetic) term in (40) ultimately becomes dominant. From this one can obtain for a cluster of fixed size the value  $L_{\text{cr}}$  at which excitations still retain their collective nature. This value can be defined as the one at which the contributions from the kinetic energy and the Coulomb interaction become equal in magnitude. We then have<sup>53</sup>

$$L_{\text{cr}} \approx 0.7 r_{\text{WS}}^{1/2} N^{1/2}. \quad (42)$$

In Ref. 55, giant resonances were investigated in an updated form of the model, in which the exchange–correlation effects were considered in a nonlocal approximation. In accordance with Ref. 55, the extension beyond the local approximation changes significantly, in the first place, the ground-state properties (though it does not reduce solely to this). In the nonlocal approximation, the single-particle potential becomes deeper, its diffuseness increases, and, most importantly, the number  $\delta N$  of electrons at  $r > R$  grows, i.e., the spill-out increases. This, in its turn, leads to a significant improvement in the description of the experimental data on the electric polarizability and the excitation energies of the giant dipole resonance. As examples, Tables III and IV give the results of calculations<sup>55</sup> for the clusters  $\text{Na}_8$  and  $\text{Na}_{20}$ .



TABLE IV. Lower and upper limits  $E_1$  and  $E_3$  for the excitation energy of the giant dipole resonance and its variance  $\sigma$  (in eV) calculated for the  $\text{Na}_8$  and  $\text{Na}_{20}$  clusters in the local (LDA) and nonlocal (NLDA) approximations for the density of the valence electrons.<sup>55</sup> For comparison, the corresponding experimental data are given.

Cluster	$(E_1)^{\text{(LDA)}}$	$(E_1)^{\text{(NLDA)}}$	$(E_3)^{\text{(LDA)}}$	$(E_3)^{\text{(NLDA)}}$	$E_{\text{exp}}$	$\sigma_{\text{LDA}}$	$\sigma_{\text{NLDA}}$	$\sigma_e$
$\text{Na}_8$	2,83	2,53	3,14	2,81	2,53	0,68	0,61	0,38
$\text{Na}_{20}$	2,91	2,67	3,14	2,97	2,46	0,59	0,65	0,37

In Refs. 54 and 56, the sum-rule method was used to obtain expressions for the moments  $m_1$ ,  $m_3$ , and  $m_{-1}$  for an external field of type  $j_L(qr)Y_{L0}$ . These results are interesting for the study of electric giant resonances with  $L \geq 0$  in reactions with electrons. In Refs. 54 and 56, estimates were made which show what the ranges are of momentum transfer  $q$  in which giant resonances of surface and bulk type will be mainly manifested, and also noncollective particle-hole excitations.

### Random-phase approximation

The RPA is a much more informative method than the sum-rule method, since it enables one to investigate cases in which there is not one collective peak but several (or many) states, these having, moreover, different natures (collective and noncollective). In practice, it is such a situation that is most often realized. It is known from experiment, for example, that even in some spherical clusters ( $\text{Na}_{20}$ ) there is an appreciable splitting of the giant dipole resonance.<sup>26,27</sup>

In the framework of the RPA, the giant dipole resonance has mainly been studied. Here, the most interesting work is the series of studies of Refs. 48, 59–63, and 72, in which this resonance was investigated in detail for a number of Na and K clusters, these being, moreover, not only neutral but also charged.

The jellium model was used for the ions, and the single-particle potential for the valence electrons was calculated in the framework of the Kohn–Sham approach, but using a modified semiclassical approximation for the kinetic-energy density.<sup>102</sup> The residual two-particle interaction had the form

$$V(|\mathbf{r}_1 - \mathbf{r}_2|) = \frac{e^2}{|\mathbf{r}_1 - \mathbf{r}_2|} + \frac{dV_{\text{ex-corr}}[n_0]}{dn_0} \delta(|\mathbf{r}_1 - \mathbf{r}_2|), \quad (43)$$

where, in accordance with Ref. 102, the exchange-correlation term  $V_{\text{ex-corr}}[n_0]$  was chosen in the form  $(r_s(\mathbf{r}) = [3/4\pi n_0(\mathbf{r})]^{1/3})$

$$dV_{\text{ex-corr}}(\mathbf{r}) = -\frac{1.222}{r_s(\mathbf{r})} - 0.0666 \ln\left(1 + \frac{11.4}{r_s(\mathbf{r})}\right). \quad (44)$$

Figure 12 gives the results of the calculations in the RPA of the photoabsorption cross section in the clusters  $\text{Na}_8$ ,  $\text{Na}_{20}$ , and  $\text{Na}_{40}$  (Ref. 61). This group of clusters is very convenient for investigating the fragmentation of the giant dipole resonance due, not to deformation of the cluster, but to configuration splitting. For, on the one hand,

these clusters have spherical shape, and, on the other hand, it is known from experiment that the giant dipole resonance has in  $\text{Na}_8$  one peak, in  $\text{Na}_{20}$  two peaks, while in  $\text{Na}_{40}$  it has been seen in the form of a broad and almost structureless distribution.<sup>26,27</sup>

In Fig. 12 we see that the calculations give a completely satisfactory description of the shape of the giant dipole resonance in all three clusters, and also the tendency for the excitation energy of the resonance to increase with increasing  $N$ . The calculations somewhat overestimate the excitation energies; this may be due to the use of the local-density approximation.<sup>55</sup>

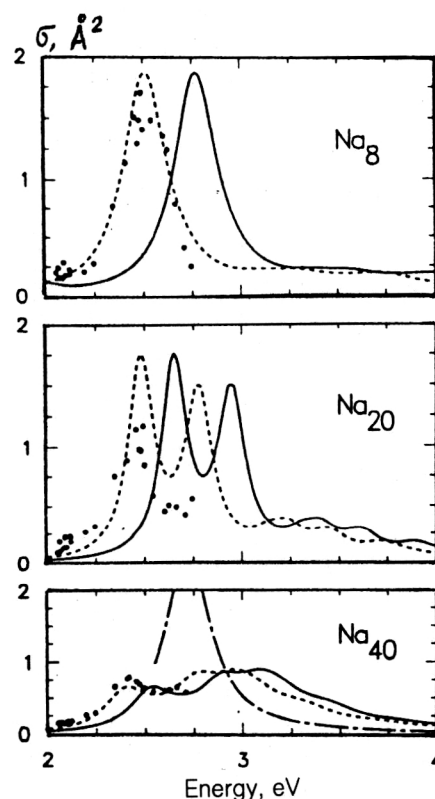


FIG. 12. Photoabsorption cross section, normalized to the number of atoms in the cluster for the clusters  $\text{Na}_8$ ,  $\text{Na}_{20}$ , and  $\text{Na}_{40}$ . The experimental data are taken from Ref. 27. The continuous curves show the results of the calculation of Ref. 61 in the RPA with subsequent “smearing” of the peaks to take into account the cluster temperature. A Lorentz distribution with peak width to peak energy ratio  $\Gamma/E=0.1$  for  $\text{Na}_8$  and  $\text{Na}_{40}$  and 0.06 for  $\text{Na}_{20}$  was used. The broken curves give the same result but with a shift along the energy scale to achieve the maximum overlap with the experimental data. The chain curve is the calculation in the sum-rule method in accordance with Ref. 26.

Analysis of the results obtained in Refs. 59, 61, and 72 reveal some interesting properties of the giant dipole resonance in metal clusters.

Because the residual interaction in metal clusters is predominantly a long-range interaction, it involves considerably more particle-hole excitations in the formation of the giant resonance than, for example, in a nucleus. Therefore, the giant resonances in neutral metal clusters are fragmented as a whole more than in nuclei.

In neutral and charged metal clusters, the fragmentation of the giant dipole resonance is very different. Compared with neutral clusters, it is significantly less in positively charged clusters (cations) and appreciably larger in negatively charged clusters (anions).<sup>72</sup> In the first place, this is explained by the appreciable rearrangement of the mean field of the cluster associated with the presence of the charge.

An interesting approach was developed in Refs. 50 and 51 on the basis of the vibrating-potential model that was originally used to study giant resonances in nuclei.<sup>103</sup> This approach leads to equations of the same form as the RPA with separable forces, but with the important difference that the form of the residual forces and the value of the strength constant are here determined from the condition of consistency of the vibrations of the density and the single-particle potential. The function  $\chi(\omega)$  of the response to an external field  $f(\mathbf{r}) = r^L Y_{LM}$  is expressed in Refs. 50 and 51 in terms of the single-particle response function

$$\chi_0(\omega) = 2 \sum_k \varepsilon_k \frac{\langle 0 | Q | k \rangle}{\omega^2 - \varepsilon_k^2} \quad (45)$$

and the force constant

$$\kappa = - \left( \int \nabla Q(\mathbf{r}) \nabla (f(\mathbf{r}) n_0(\mathbf{r})) d\mathbf{r} \right)^{-1} \quad (46)$$

by means of the RPA equation

$$\chi(\omega) = \frac{\chi_0(\omega)}{1 - \kappa \chi_0(\omega)}. \quad (47)$$

The operator of the residual interaction has the form

$$Q(\mathbf{r}) = \nabla V_0(\mathbf{r}) \nabla f(\mathbf{r}) + \int \frac{\nabla n_0(\mathbf{r}') \nabla f(\mathbf{r}')}{|\mathbf{r} - \mathbf{r}'|} d\mathbf{r}', \quad (48)$$

where

$$V_0(\mathbf{r}) = \left( \frac{dv_{\text{ex-corr}}[n]}{dn} \right)_{n=n_0}. \quad (49)$$

A shortcoming of the approach of Refs. 50 and 51 compared with Refs. 59–63 is the separable nature of the residual interaction. On the other hand, this feature of the approach of Refs. 50 and 51 greatly simplifies the calculations, and this is important in the study of deformed clusters, and also large clusters.

### Linear response-function method

Compared with the methods considered above, the linear response-function method<sup>65–69</sup> is the most rigorous,

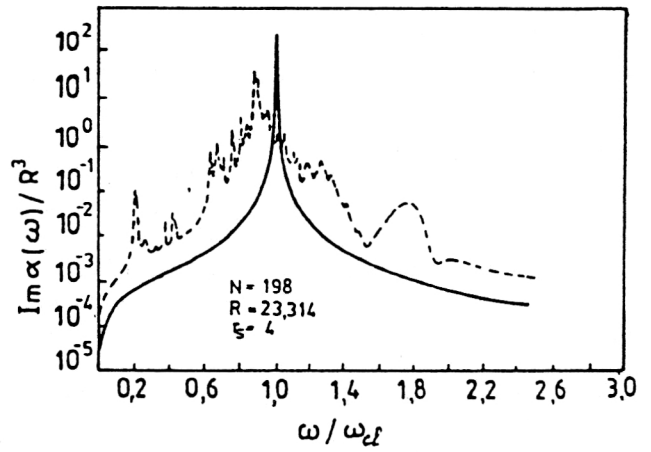


FIG. 13. Imaginary part of the dynamic polarizability  $\alpha(\omega)$  in units of  $R^3$ , calculated in the framework of the linear response function.<sup>65</sup> The frequency is given in units of  $\omega_{cl} = \omega_p/\sqrt{3}$  for the Na clusters. The curve obtained in the local Drude theory is given for comparison.

since it permits one to make self-consistent calculations. The ion density is treated in the jellium model. The local-density approximation is used for the valence electrons.

In the method,<sup>65–69</sup> the induced electron density  $n_{\text{ind}}(\mathbf{r}, \omega)$  in a cluster in an oscillating external field  $V_{\text{ex}}(\mathbf{r}, \omega) e^{-i\omega t}$  can be expressed in terms of the response function  $\chi(\mathbf{r}, \mathbf{r}', \omega)$ :

$$n_{\text{ind}}(\mathbf{r}, \omega) = \int d\mathbf{r}' \chi(\mathbf{r}, \mathbf{r}', \omega) V_{\text{ex}}(\mathbf{r}, \omega). \quad (50)$$

In the time-dependent local-density approximation (TDLDA) we have for the response function the integral equation

$$\begin{aligned} \chi(\mathbf{r}, \mathbf{r}', \omega) = & \chi_0(\mathbf{r}, \mathbf{r}', \omega) \\ & + \iint d\mathbf{r}'' d\mathbf{r}''' \chi_0(\mathbf{r}, \mathbf{r}'', \omega) K(\mathbf{r}'', \mathbf{r}''') \chi(\mathbf{r}''', \mathbf{r}', \omega), \end{aligned} \quad (51)$$

which is obtained from the condition of consistency of the single-particle response function and the effective potential:

$$n_{\text{ind}}(\mathbf{r}, \omega) = \int d\mathbf{r}' \chi_0(\mathbf{r}, \mathbf{r}', \omega) V_{\text{eff}}(\mathbf{r}, \omega). \quad (52)$$

In (51)–(52),

$$V_{\text{eff}}(\mathbf{r}, \omega) = V_{\text{ex}}(\mathbf{r}, \omega) + \int d\mathbf{r}' K(\mathbf{r}, \mathbf{r}') n_{\text{ind}}(\mathbf{r}', \omega), \quad (53)$$

$$K(\mathbf{r}, \mathbf{r}') = \frac{2}{|\mathbf{r} - \mathbf{r}'|} + \frac{dV_{\text{ex-corr}}[n]}{dn} \delta(\mathbf{r} - \mathbf{r}'). \quad (54)$$

The single-particle response function can be expressed in terms of the retarded Green's functions of the ground state of the Hamiltonian.

As an example, Fig. 13 shows the results<sup>65</sup> of a calculation in the response-function method of the imaginary part of the cluster dynamic polarizability, which is related to the photoabsorption cross section by

$$\sigma(\omega) = 4\pi\omega \operatorname{Im} \alpha(\omega). \quad (55)$$

The figure clearly demonstrates excitations of different types: single-particle, and also collective surface and volume type. It can be seen that, compared with the classical frequencies of the surface and volume resonances, which are, respectively,  $\omega_p/\sqrt{3}$  and  $\omega_p$ , the self-consistent calculations give underestimated frequencies of the surface resonance and somewhat overestimated frequencies of the volume resonance. In Ref. 65, these differences are explained by the competition of two effects: 1) quantization of the single-particle spectrum, which leads to a raising of the frequencies compared with the classical treatment; 2) the spill-out effect, which lowers the frequencies. It is clear that for the surface resonance the second effect will be dominant, while for the volume resonances it will be the first. This explains the differences.

### Kresin's approach

Kresin's approach<sup>9,57,58</sup> is attractive in that analytic expressions, which greatly facilitate the analysis, can be obtained for several properties of the giant dipole resonance. Conceptually, the approach is based on Ref. 107. The essence of the method is as follows. One takes equations of self-consistent type for an electron in an external field, written down in the RPA (as in the response-function method). On the basis of a semiclassical argument, it is asserted that in the case of dipole fields the main contribution to the equations is made by single-particle transitions between neighboring levels  $\lambda$  and  $\lambda'$ , the energy  $|\varepsilon_\lambda - \varepsilon_{\lambda'}| \approx 0.1-0.3$  eV of which is much less than the energy  $\omega \gg 2$  eV of the giant dipole resonance. As a result, one can expand the equations, using  $(\varepsilon_\lambda - \varepsilon_{\lambda'})/\omega$  as a small parameter and retaining only the first-order terms. If it is also borne in mind that the derivative of the electron density in a metal cluster has a peak on its boundary, then one can use an additional expansion in the region  $r \approx R$ , retaining only the terms linear in  $r - R$ . As a result, even when diffuseness on the cluster boundary is taken into account (spill-out), one can obtain a simple analytic expression for the eigenfrequencies (the external field is zero) of the collective dipole excitations:<sup>9,57</sup>

$$6\left(\frac{\omega_\pm}{\omega_p}\right)^2 = 3g(R) + 1 \pm \{[3g(R) - 1]^2 + 24q(1 - 3g)\}^{1/2}, \quad (56)$$

where

$$g(r) = n_0(r)/n^+, \quad (57)$$

$$q = 1/R \int_{r>R} dr g(r). \quad (58)$$

Obviously,  $q$  is a measure of the spill-out effect. It can be seen from (56) that  $g(R)$  and  $q$  are the only input parameters. To determine them, it is sufficient to know the density  $n_0(r)$  of the valence electrons in the ground state. In Kresin's approach, the electron density is usually calculated in the Thomas-Fermi approximation. However, in

contrast to the case of atoms, there is here no need to solve differential equations. It is shown in Refs. 9 and 108 that, by virtue of the comparatively uniform distribution of the positive charge in metal clusters, analytic expressions can again be obtained for  $g(R)$  and  $q$ .<sup>108</sup> These expressions do not contain any adjustable parameters.

Equation (56) has two solutions:  $\omega_-$  and  $\omega_+$ . Their physical meaning becomes clear if one considers the limiting case of a cluster with a sharp edge and with  $n_0(r) = n^+$ . Then there is no spill-out, and for the input quantities we have  $q=0$ ,  $g(r)=1$  for  $r < R$  and  $g(r)=0$  for  $r > R$ . This case corresponds to the classical limit that holds for large clusters. As a result,  $\omega_- = \omega_p/\sqrt{3}$  and  $\omega_+ = \omega_p$ , and these are none other than the frequencies of the characteristic dipole vibrations of surface and volume type in a classical metallic particle.<sup>101</sup> We emphasize that in the above we are, as a rule, considering a giant dipole resonance of surface type. Practically all the experimental data on dipole excitations in metal clusters relate to them. The volume dipole resonance is at a higher energy (for sodium clusters, above the ionization threshold), and experimental data on them in metal clusters are extremely sparse.

In real clusters of not too large size, the volume and surface dipole resonances are partly mixed, although they basically retain their individuality. As can be seen from Eq. (56), this mixing is to a large degree due to the spill-out effect. In Refs. 9 and 58, it is asserted that it is precisely the mixing of the surface and volume branches of the giant dipole resonance which is responsible for the fact that in some small clusters the strength of the  $E1$  transitions obtained in the photoabsorption reaction is manifestly insufficient to exhaust the Thomas-Reiche-Kuhn sum rule. Indeed, whereas in a solid the volume (plasma) dipole vibrations have a strictly longitudinal nature and cannot be excited by  $\gamma$  rays having transverse polarization, this is possible in metal clusters because of the small size of the systems and, accordingly, the importance of surface effects. In small metal clusters, the volume branch of the giant dipole resonance has an admixture of the surface branch, as a result of which it can be excited in the photoabsorption reaction, taking to itself some of the  $E1$  strength. This part of the  $E1$  strength is concentrated at a higher energy, is not so clearly expressed, and is evidently not captured by the measurements, which are mainly aimed at the region of excitation of the surface branch of the dipole resonance. However, we note here that an additional reason for the smallness of the  $E1$ -transition strength extracted from experiment could also be ordinary fragmentation (configuration splitting) of dipole excitations, as a consequence of which some of the  $E1$  strength can be in the "base."

Another interesting effect investigated in Kresin's approach is the splitting of the surface dipole resonance into two peaks of comparable intensity in spherical clusters.<sup>9,58</sup> It was shown that this effect is due to interaction of the collective excitation with the single-particle excitation, which has a similar energy. The nature of this effect is the same as for the well-known Fermi resonance in molecules.

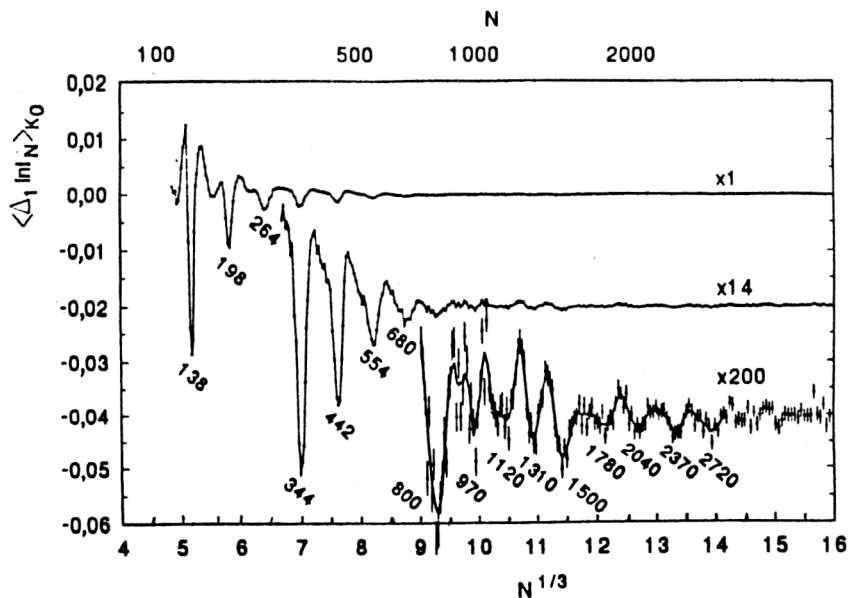


FIG. 14. Experimental data from which the values of the magic numbers for Na clusters were deduced in Refs. 23 and 24.

## 8. LARGE CLUSTERS AND SUPERSHELLS

From the time of the discovery in 1984 of shells in metal clusters, there has been unbroken discussion of the questions of how many shells of "nuclear" type can in principle exist in such clusters and of the limiting number of atoms at which the mean field disappears, as it does in atoms and nuclei. Without going into the history of the development of these questions during the last seven years, we turn directly to the present situation.

The main experiments in this direction were made in Copenhagen<sup>23,24</sup> and Stuttgart.<sup>25</sup> At the present time, there are already experimental data on the existence, in Na clusters with up to 3000 atoms, of at least 23 shells of "nuclear" type.<sup>23,24</sup> Figure 14 gives the experimental data from which the magic numbers corresponding to these shells were extracted in Refs. 23 and 24. It can be seen from the figure that the larger is the cluster, the more complicated are the combinations of measured intensities that must be used to find the magic numbers and, accordingly, the lower is the reliability of the result. In principle, the measurements suggest that shells of nuclear type survive in Na clusters at least up to  $N \approx 3000$ . However, such a conclusion must as yet be treated with sufficient caution. The point is that independent measurements of the group at Stuttgart,<sup>25</sup> made for relatively cold Na clusters ( $T \approx 100^\circ\text{K}$ ) with  $N$  up to 20 000, showed that at  $N \approx 1400$  there is a rearrangement of the cluster structure, namely, some of the magic numbers corresponding to shells of nuclear type go over into magic numbers corresponding to an icosahedral structure. Thus, at the moment one can say confidently that the shells of nuclear type survive in Na clusters only for clusters with  $N \leq 1400$ . It may also be that the critical value of  $N$  at which the structural transition takes place depends on a number of conditions (for example, the temperature of the clusters at the end of the beam in the experiment of Ref. 25 was much lower than in the experiments of Refs. 23 and 24).

Table V gives a list of experimental data from Refs. 23–25 on magic numbers in Na clusters, and also corresponding theoretical values obtained from calculations with the single-particle Woods–Saxon potential.<sup>22</sup> In Ref. 22, the total energy of the system was calculated as the sum of the single-particle energies corresponding to occupied states. From the total energy, the smooth part  $E_{av} = -4.34N + 2.96N^{2/3}$  eV was then subtracted. In this way, the shell part of the binding energy of the system was found. The values of  $N$  for which the absolute values of the shell energy had a maximum were assumed to be magic. It can be seen from the table that the calculations of Ref. 22 agree well with the experimental data. It should be mentioned that for the large clusters (with  $N > 138$ ) the calculations were made before the experimental data appeared.

We now consider supershells in metal clusters. As we have already said, supershells were first predicted theoretically,<sup>21,22</sup> and then discovered experimentally.<sup>23</sup> In accordance with Refs. 21 and 22, supershells can be manifested only in systems containing sufficiently many particles (of the order of a thousand). Neither an atom nor a nucleus will do. The only currently known objects in which one can study supershells are metal clusters.

To determine what is meant by supershells, consider Figs. 15 and 16, which demonstrate how, in accordance with the calculations of Ref. 21, supershells must be manifested in the dependence of the density of the electrons on their wave number (excitation energy), and also in the dependence of the shell energy on  $N$ . It can be seen from the figures that in both cases oscillations of low frequency are superimposed on oscillations with high frequency (each oscillation corresponds to one shell), i.e., there is an envelope of the high-frequency oscillations. Such an envelope is called a supershell. Figure 17 shows how a supershell is manifested experimentally.

A qualitative explanation of the nature of supershells,



TABLE V. Theoretical<sup>22</sup> and experimental<sup>23-25</sup> values of the magic numbers in Na clusters.

Shell number	Theory (Ref. 22)	Experiment <sup>23,24</sup>	Experiment <sup>25</sup>
1	2	2	2
2	8	8	8
3	20	20	18/20
4	40	40	34/40
5	58/68	58	58
6	92	92	90/92
7	138	138	138
8	198	196	198±2
9	254/268	264	263±5
10	338	344	341±5
11	440	442	443±5
12	562	554	557±5
13	694	680	700±15
14	832	800	840±15
15	1012	970	1040±20
16	1100	1120	—
17	1216	—	1220±20
18	1314	1310	1430±20
19	1516	1500	1980*
20	1760	1780	2820*
21	2048	2040	3800*
22	2334/2368	2370	5070*
23	2672	2720	6550*
24	3028		8170*
25	3438		10200*
26	3848		12500*
27	4154		15100*
28			18000*
29			21300*

strengthened then by calculations, was given in Refs. 21 and 22. It is well known that with increasing number of particles in a quantum system the energy separation between shells decreases. On the other hand, metal clusters have a certain temperature. It is clear that with increasing number of atoms in a cluster the energy separation between

shells becomes equal in order of magnitude at some stage to the temperature. Then as a result of the temperature there will be a smearing of the shells.

It was shown in Ref. 104 that the shells in nuclei, etc., which are a characteristic property of quantum systems, have a classical analog in the form of periodic closed orbits in the motion of a particle in a spherical vibrator. These

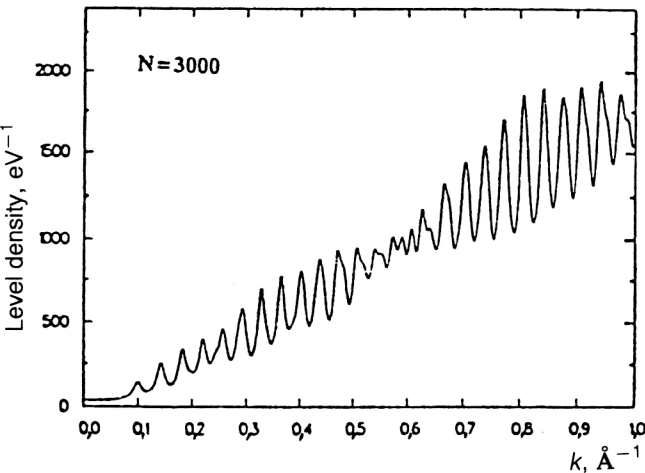


FIG. 15. Density of single-particle levels calculated in Ref. 21 with Woods-Saxon potential for the Na<sub>3000</sub> cluster. The abscissa gives the wave number  $k$ , which is related to the cluster excitation energy  $E$  by  $k = (2m(E - V_0))^{1/2}/\hbar$ , where  $V_0 = -6.0$  eV.

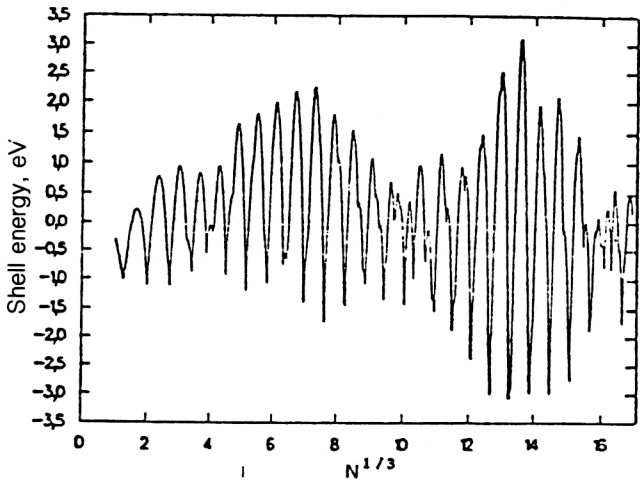


FIG. 16. Shell part of the binding energy of the Na cluster as a function of  $N^{1/3}$  (Ref. 23).

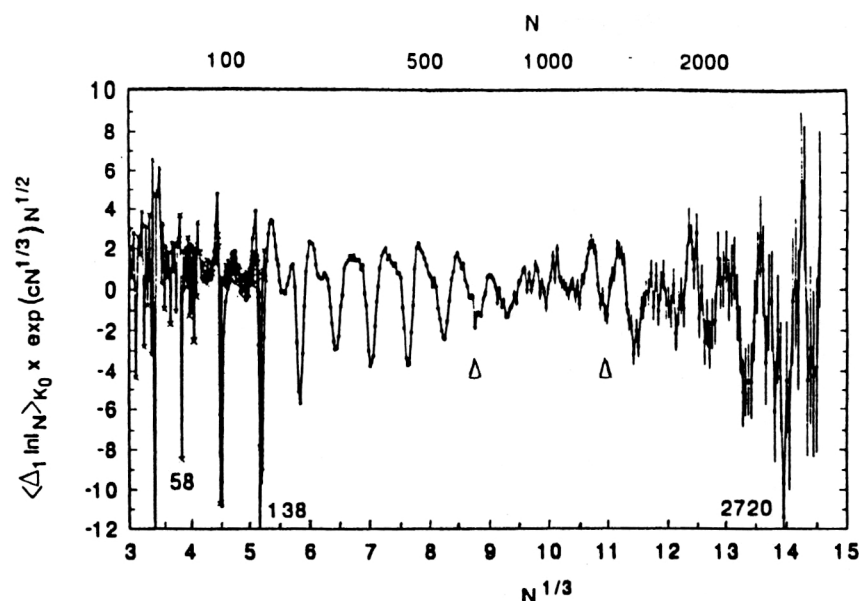


FIG. 17. Experimental data<sup>23</sup> demonstrating the manifestation of supershells in Na clusters.

orbits have different shapes and lengths. The simplest of them are shown in Fig. 18. Inclusion of a temperature leads to smearing and entangling of these orbits, and this happens more strongly, the longer the orbit. As a result, only the simplest orbits survive. As was shown in Ref. 104, these will be the orbits of triangular and square shape. These orbits can be regarded as two vibrations with nearly equal amplitudes and frequencies. In this case, as is well known, beats occur, i.e., low-frequency oscillations are superimposed on the high-frequency oscillations. This is the essence of supershells. From what has been said above, it also becomes clear why the system must have sufficiently many particles if supershells are to be manifested. It is interesting to note that supershells are, essentially, the first experimental confirmation of the ideas advanced in Ref. 104. In this respect, metal clusters are extremely interesting objects for investigating the connection between the properties of the quantum and classical systems.

## 9. CONCLUSIONS

The aim of this review was to acquaint nuclear physicists with a young and now rapidly developing field—the physics of metal clusters. We have given the basic data on them, and we have also discussed some of the directions that are currently most interesting: shells in metal clusters, deformation, giant resonances, and supershells.

From the presented material it is evident that metal clusters do indeed have much in common with nuclei, and in this respect they are very attractive objects for study for nuclear physicists. In the first place, this applies to theoreticians. Many theoretical models and approaches developed in nuclear theory have already been transferred to the physics of these clusters. Many well-known nuclear physicists have begun active work in this field. It is possible that after some time there will be a feedback—developments in the physics of metal clusters may assist the development of

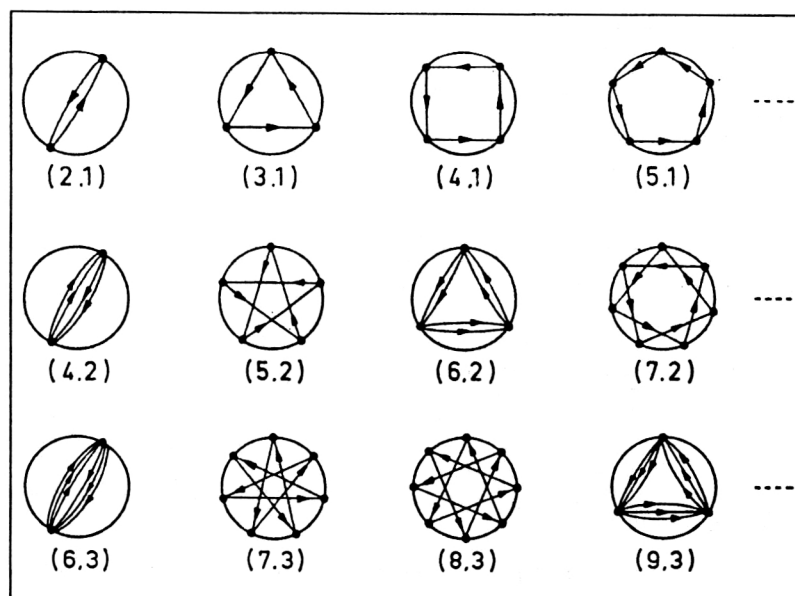


FIG. 18. Examples of closed trajectories of the motion of a particle in a spherical vibrator.<sup>104</sup>

new methods for investigating nuclei and make it possible to reexamine, from new positions, effects in nuclei that have apparently already been studied.

Specialists in experimental nuclear physics can also be included in the investigation of metal clusters. In the first place, this applies to someone working with lasers. As we have already said, lasers can be used effectively to obtain beams of clusters. For this purpose, one can use heavy ions. Elastic scattering of thermal neutrons could be used to investigate the ion lattice of a cluster and its shape.

One might get the impression that in the early stages of its development the physics of metal clusters simply copies nuclear physics. In part, this is indeed the case. Nuclear physics possesses tremendous potential. The desire to use this potential in a new field is entirely natural and sensible. However, we emphasize that this process does not reduce to trivial copying. It brings new knowledge, which, moreover, is of a fundamental nature. It is sufficient to mention the discovery of supershells and the very interesting information on the possible number of shells in a Fermi system.

It is worth saying some words on the prospects for investigations of metal clusters. As a general remark, we would like to mention that in some respects metal clusters are more convenient objects for study of the global properties of Fermi systems than nuclei; for in them the interaction is known, they can have many more particles than nuclei, and they can be both charged and neutral. If we speak of definite directions, the most promising ones are the possibility of pairing in the clusters (pairing mechanisms, connection with high-temperature superconductivity), deformation (new shapes, global tendencies, deformation in clusters with a large number of particles), magnetic giant resonances (because the spin-orbit coupling is weak in metal clusters, the orbital and spin modes in them must, in contrast to nuclei, be decoupled), and charged and mixed clusters. The clusters are also interesting from the point of view of practical applications. There are here interesting possibilities for the physics of aerosols, powder technologies, catalysis, superconductivity, alloy physics, etc.

More and more new directions are appearing in the physics of metal clusters. Some of them have been described in this review very briefly. It is hoped later to write a more extensive review, including in it sections such as pairing in metal clusters, fission, temperature in the clusters, mixed clusters, the basic experimental methods, etc. It is also planned to give information on some other exotic objects that also have much in common with nuclei: helium clusters,<sup>8,109</sup> fullerenes,<sup>8,110</sup> and quantum points.<sup>111</sup> The physics of these systems developed comparatively recently and is currently undergoing rapid development.

- <sup>5</sup> I. Katakuse, T. Ichihara, Y. Fujita *et al.*, *Int. J. Mass Spectrom. Ion Phys.* **67**, 229 (1986); **69**, 109 (1986).
- <sup>6</sup> W. Ekardt, *Phys. Rev. B* **29**, 1558 (1984).
- <sup>7</sup> W. A. de Heer, W. D. Knight, M. Y. Chou *et al.*, *Solid State Phys.* **40**, 93 (1987).
- <sup>8</sup> S. Bjørnholm, *Contemp. Phys.* **31**, 309 (1990).
- <sup>9</sup> V. Kresin, submitted to *Phys. Rep.* (1992).
- <sup>10</sup> V. O. Nesterenko, *Proc. of the Fourth Intern. Seminar on Nuclear Physics* (Amalfi, Italy, 1992).
- <sup>11</sup> A. S. Davydov, *Quantum Mechanics* (Pergamon Press, Oxford, 1965) [Russ. original, Fizmatgiz, Moscow, 1963].
- <sup>12</sup> S. Arvati *et al.*, *Nuovo Cimento* **D7**, 1063 (1989).
- <sup>13</sup> A. vom Felde, J. Fink, and W. Ekardt, *Phys. Rev. Lett.* **61**, 2249 (1988).
- <sup>14</sup> H. Gohlich, T. Lange, T. Bergmann, and T. P. Martin, *Phys. Rev. Lett.* **65**, 748 (1990).
- <sup>15</sup> K. Clemenger, *Phys. Rev. B* **32**, 1359 (1985).
- <sup>16</sup> O. Echt, K. Sattler, and E. Recknagel, *Phys. Rev. Lett.* **47**, 1121 (1981).
- <sup>17</sup> O. Echt *et al.*, *25th Faraday Symposium on Large Phase Gas Clusters* (University of Warwick, 1989).
- <sup>18</sup> J. Farges *et al.*, *J. Chem. Phys.* **84**, 3491 (1986).
- <sup>19</sup> J. B. Hopkins, P. R. R. Langridge-Smith, M. D. Morse, and R. E. Smalley, *J. Chem. Phys.* **78**, 1627 (1983).
- <sup>20</sup> D. Tomanek and M. A. Schluter, *Phys. Rev. Lett.* **67**, 2331 (1991).
- <sup>21</sup> H. Nishioka, *Z. Phys. D* **19**, 19 (1991).
- <sup>22</sup> H. Nishioka, K. I. Hansen, and B. R. Mottelson, *Phys. Rev. B* **42**, 9377 (1990).
- <sup>23</sup> J. Pedersen, S. Bjørnholm, J. Borggreen *et al.*, *Nature* **353** (1991).
- <sup>24</sup> S. Bjørnholm *et al.*, *Z. Phys. D* **19**, 47 (1991).
- <sup>25</sup> T. P. Martin, T. Bergmann, H. Gohlich, and T. Lange, *Chem. Phys. Lett.* **172**, 209 (1990).
- <sup>26</sup> K. Selby *et al.*, *Phys. Rev. B* **40**, 5417 (1989).
- <sup>27</sup> K. Selby *et al.*, *Z. Phys. D* **19**, 43 (1991).
- <sup>28</sup> V. O. Nesterenko and N. Yu. Shirikova, *JINR, Dubna* (1993) (to be published).
- <sup>29</sup> V. V. Pashkevich and S. Frauendorf, submitted to *Z. Phys. D* (1992).
- <sup>30</sup> I. Hamamoto, B. Mottelson, H. Xie, and X. Z. Zhang, *Z. Phys. D* **21**, 163 (1991).
- <sup>31</sup> I. Katakuse, H. Ito, and T. Ichihara, *Int. J. Mass. Spectrom. Ion Phys.* **97**, 47 (1990).
- <sup>32</sup> T. P. Martin *et al.*, submitted to *Chem. Phys. Lett.* (1992).
- <sup>33</sup> V. M. Strutinsky, *Nucl. Phys.* **95**, 420 (1967).
- <sup>34</sup> V. M. Strutinskii, *Yad. Fiz.* **3**, 614 (1966) [*Sov. J. Nucl. Phys.* **3**, 449 (1966)].
- <sup>35</sup> M. Nakamura *et al.*, *Techn. Rep. of ISSP, Ser. A*, n.2259 (1990).
- <sup>36</sup> E. Lipparini and A. Vitturi, *Z. Phys. D* **17**, 57 (1990).
- <sup>37</sup> F. Garcias, J. A. Alonso, J. M. Lopez, and M. Barranco, *Phys. Rev. B* **43**, 9459 (1991).
- <sup>38</sup> V. A. Rubchenya, *Lect. Notes Phys.* **404**, 98 (1991); *Proc. of the Intern. Conf. on Nuclear Physics. Concepts in Study of Atomic Cluster Physics*, edited by R. Schmidt, H. O. Lutz, and R. Dreizler (Bad Honned FRG, 1991).
- <sup>39</sup> M. Barranco *et al.*, *Z. Phys. D* **22**, 659 (1992).
- <sup>40</sup> E. Lipparini, Preprint UTF239, Trento (1991).
- <sup>41</sup> K. E. Schriver *et al.*, *Phys. Rev. Lett.* **64**, 2539 (1990).
- <sup>42</sup> K. Laiting *et al.*, *Z. Phys. D* **13**, 161 (1989).
- <sup>43</sup> M. M. Kappes *et al.*, *Chem. Phys. Lett.* **143**, 251 (1988).
- <sup>44</sup> J. L. Persson, Thesis, Univ. of California, Los Angeles (1991).
- <sup>45</sup> Z. Penzar and W. Ekardt, *Z. Phys. D* **19**, 109 (1991).
- <sup>46</sup> J. Tiggesbaumer *et al.*, *Chem. Phys. Lett.* **190**, 42 (1992).
- <sup>47</sup> J. N. Parks and S. A. McDonald, *Phys. Rev. Lett.* **62**, 2301 (1989).
- <sup>48</sup> C. Yannouleas and R. A. Broglia, *Ann. Phys. (N.Y.)* **217**, 105 (1992).
- <sup>49</sup> G. Bertsch and W. Ekardt, *Phys. Rev. B* **32**, 7659 (1985).
- <sup>50</sup> E. Lipparini and S. Stringari, *Z. Phys. D* **18**, 193 (1991).
- <sup>51</sup> E. Lipparini, Preprint UTF200, Trento (1991).
- <sup>52</sup> M. Brack, *Phys. Rev. B* **39**, 3533 (1989).
- <sup>53</sup> Ll. Serra, F. Garcias, M. Barranco *et al.*, *Phys. Rev. B* **39**, 8247 (1989).
- <sup>54</sup> Ll. Serra, F. Garcias, M. Barranco *et al.*, *Phys. Rev. B* **41**, 3434 (1990).
- <sup>55</sup> A. Rubio, L. C. Balbas, Ll. Serra, and M. Barranco, *Phys. Rev. B* **42**, 10 950 (1990).
- <sup>56</sup> Ll. Serra, F. Garcias, N. Barberan *et al.*, *Z. Phys. D* **19**, 89 (1991).
- <sup>57</sup> V. Kresin, *Phys. Rev. B* **42**, 3247 (1990).
- <sup>58</sup> V. Kresin, *Z. Phys. D* **19**, 105 (1991).

<sup>1</sup> W. D. Knight, K. Clemenger, W. A. de Heer *et al.*, *Phys. Rev. Lett.* **52**, 2141 (1984).

<sup>2</sup> W. D. Knight, W. A. de Heer, K. Clemenger, and W. A. Saunders, *Solid State Commun.* **53**, 445 (1985).

<sup>3</sup> W. D. Knight, K. Clemenger, W. A. de Heer, and W. A. Saunders, *Phys. Rev. B* **31**, 2539 (1985).

<sup>4</sup> W. A. Saunders, K. Clemenger, W. A. de Heer, and W. D. Knight, *Phys. Rev. B* **32**, 1366 (1985).

- <sup>59</sup>C. Yannouleas, R. A. Broglia, M. Brack, and P. F. Bortignon, *Phys. Rev. Lett.* **63**, 255 (1989).
- <sup>60</sup>C. Yannouleas, J. M. Pacheco, and R. A. Broglia, *Phys. Rev. B* **41**, 6088 (1990).
- <sup>61</sup>C. Yannouleas and R. A. Broglia, *Phys. Rev. A* **44**, 5793 (1991).
- <sup>62</sup>C. Yannouleas and R. A. Broglia, *Europhys. Lett.* **15**, 843 (1991).
- <sup>63</sup>R. A. Broglia, J. M. Pacheco, and C. Yannouleas, *Phys. Rev. B* **44**, 5901 (1991).
- <sup>64</sup>J. M. Pacheco, R. A. Broglia, and B. R. Mottelson, *Z. Phys. D* **21**, 289 (1991).
- <sup>65</sup>W. Ekardt, *Phys. Rev. Lett.* **52**, 1925 (1984).
- <sup>66</sup>W. Ekardt, *Phys. Rev. B* **31**, 6360 (1985).
- <sup>67</sup>W. Ekardt, *Phys. Rev. B* **36**, 4483 (1987).
- <sup>68</sup>Z. Penzar, W. Ekardt, and A. Rubio, *Phys. Rev.* **42**, 5040 (1990).
- <sup>69</sup>W. Ekardt and Z. Penzar, *Phys. Rev. B* **42**, 1322 (1991).
- <sup>70</sup>B. Wassermann and W. Ekardt, *Z. Phys. D* **19**, 97 (1991).
- <sup>71</sup>N. Barberan and J. Bausells, *Phys. Rev. B* **31**, 6354 (1985).
- <sup>72</sup>C. Yannouleas, submitted to *Chem. Phys. Lett.* (1992).
- <sup>73</sup>G. F. Bertsch, N. Oberhofer, and S. Stringari, *Z. Phys. D* **20**, 123 (1991).
- <sup>74</sup>M. Brack, O. Genzken, and K. Hansen, *Z. Phys. D* **19**, 51 (1991).
- <sup>75</sup>C. Yannouleas, P. Jena, and S. N. Khanna, *Contributions to the Intern. Symposium on Physics and Chemistry of Finite Systems. From Clusters to Crystals* (Richmond, Virginia, USA, 1991).
- <sup>76</sup>W. Ekardt and Z. Penzar, *Phys. Rev. B* **38**, 4273 (1988).
- <sup>77</sup>M. Ya. Amus'ya and V. R. Shaginyan, Preprint No. 1690 [in Russian], Leningrad Institute of Nuclear Physics, Leningrad (1991).
- <sup>78</sup>S. V. Tolokonnikov and S. A. Fayans, *Pis'ma Zh. Eksp. Teor. Fiz.* **35**, 403 (1982) [*JETP Lett.* **35**, 499 (1982)].
- <sup>79</sup>F. Iachello, E. Lipparini, and A. Ventura, *Phys. Rev. B* **45**, 4431 (1992).
- <sup>80</sup>M. Seidl, M. E. Spina, and M. Brack, *Z. Phys. D* **19**, 101 (1991).
- <sup>81</sup>T. Bastug *et al.*, *Z. Phys. D* **22**, 641 (1991).
- <sup>82</sup>M. Koskinen, P. O. Lipas, E. Hammaren, and M. Manninen, Preprint, University of Jyväskylä, JYFL 6/92 (1992).
- <sup>83</sup>M. Koskinen *et al.*, *Lect. Notes Phys.* **404**, 335 (1991); *Proc. of the Intern. Conf. on Nuclear Physics. Concepts in Study of Atomic Cluster Physics*, edited by R. Schmidt, H. O. Lutz, and R. Dreizler (Bad Honnef FRG, 1991); Preprint, University of Jyväskylä JYFL 6/92 (1992).
- <sup>84</sup>P. Hohenberg and W. Kohn, *Phys. Rev.* **136**, B864 (1964).
- <sup>85</sup>W. Kohn and L. J. Sham, *Phys. Rev.* **140**, A1133 (1965).
- <sup>86</sup>N. D. Lang and W. Kohn, *Phys. Rev. B* **1**, 4555 (1970).
- <sup>87</sup>D. R. Snider and R. S. Sorbello, *Phys. Rev. B* **28**, 5702 (1983).
- <sup>88</sup>G. Nilsson, *K. Dan. Vidensk. Selsk. Mat.-Fys. Medd.* **29**, No. 16 (1955).
- <sup>89</sup>C. Gustafson, I. L. Lamm, and G. Nilsson, *Ark. Phys.* **36**, 613 (1967).
- <sup>90</sup>M. Y. Chou, A. Cleland, and M. L. Cohen, private communication.
- <sup>91</sup>G. S. Anagnostatos, *Phys. Lett.* **154A**, 169 (1991).
- <sup>92</sup>G. S. Anagnostatos, *Phys. Lett.* **157A**, 65 (1991).
- <sup>93</sup>J. Mansikka-aho, M. Manninen, and E. Hammaren, *Z. Phys. D* **21**, 271 (1991).
- <sup>94</sup>F. A. Gareev *et al.*, *Fiz. Elem. Chastits At. Yadra* **4**, 357 (1973) [*Sov. J. Part. Nucl.* **4**, 148 (1973)].
- <sup>95</sup>N. Lo Iudice and F. Palumbo, *Phys. Rev. Lett.* **41**, 1532 (1978).
- <sup>96</sup>P. E. Batson, *Surf. Sci.* **156**, 720 (1985).
- <sup>97</sup>J. Sprösser-Prou, A. vom Felde, and J. Fink, *Phys. Rev. B* **40**, 5799 (1989).
- <sup>98</sup>E. Lipparini and S. Stringari, *Phys. Rep.* **175**, 103 (1989).
- <sup>99</sup>M. Casas and J. Martorell, *Nucl. Phys.* **A490**, 329 (1988).
- <sup>100</sup>O. Bohigas *et al.*, *Phys. Rep.* **51**, 267 (1979).
- <sup>101</sup>G. Mie, *Ann. Phys. (N.Y.)* **25**, 377 (1908).
- <sup>102</sup>O. Gunnarsson and B. I. Lundquist, *Phys. Rev. B* **13**, 4274 (1976).
- <sup>103</sup>E. Lipparini and S. Stringari, *Nucl. Phys.* **A371**, 430 (1981).
- <sup>104</sup>R. Balian and C. Bloch, *Ann. Phys. (N.Y.)* **69**, 76 (1971).
- <sup>105</sup>D. E. Beck, *Phys. Rev. B* **30**, 6935 (1984).
- <sup>106</sup>V. Bonacic-Koutecky, P. Fantucci, and J. Koutecky, *Chem. Rev.* **91**, 1035 (1991).
- <sup>107</sup>A. A. Lushnikov and A. J. Simonov, *Z. Phys.* **270**, 17 (1974).
- <sup>108</sup>V. Kresin, *Phys. Rev. B* **38**, 3741 (1988).
- <sup>109</sup>S. Stringari, *Z. Phys. D* **20**, 219 (1991).
- <sup>110</sup>R. E. Smalley, *Acc. Chem. Res.* **25**, 3, 98 (1992).
- <sup>111</sup>*Proc. of the Eighth Conf. on the Electronic Properties of Two-Dimensional Systems*, *Surf. Sci.* **229** (1990).
- <sup>112</sup>B. R. Mottelson, *Clustering Phenomena in Atoms and Nuclei. Springer Series in Nucl. and Phys.: Intern. Conf. on Nucl. and Atomic Clusters* (Turku, Finland, 1991), p. 571.

Translated by Julian B. Barbour